Direct Stability Analysis of Electric Power Systems Using Energy Functions: Theory, Applications, and Perspective

HSIAO-DONG CHIANG, SENIOR MEMBER, IEEE, CHIA-CHI CHU, STUDENT MEMBER, IEEE, AND GERRY CAULEY, SENIOR MEMBER, IEEE

Invited Paper

Stability analysis programs are a primary tool used by power system planning and operating engineers to predict the response of the system to various disturbances. Important conclusions and decisions are made based on the results of stability studies. The conventional method of analyzing stability is to calculate the transient behavior of generators due to a given disturbance. By examining the behavior of generators, one determines whether stability has been maintained or lost. In contrast, direct methods of stability analysis identify whether or not the system will remain stable once the disturbance is removed by comparing it with a calculated threshold value. Direct methods not only avoid the time-consuming solutions required in the conventional method, but also provide a quantitative measure of the degree of system stability. This additional information makes direct methods very attractive when the relative stability of different plans must be compared or when stability limits must be calculated quickly.

This paper presents a theoretical foundation of direct methods for both network-reduction and network-preserving power system models. In addition to an overview, new results are offered. A systematic procedure of constructing energy functions for both network-reduction and network-preserving power system models is proposed. An advanced method, called the BCU method, of computing the controlling unstable equilibrium point is presented along with its theoretical foundation. Numerical solution algorithms capable of supporting on-line applications of direct methods are provided. Practical demonstrations of using direct methods and the BCU method for on-line transient stability assessments on two power systems are described. Further possible improvements, enhancements and other applications of direct methods are outlined.

I. INTRODUCTION

By nature, a power system is continually experiencing disturbances. These may be classified as *event disturbances* and *load disturbances*. Event disturbances include generator outages, short-circuits caused by lightning or other fault conditions, sudden large load changes, or a combination of such events. Event disturbances usually lead to a change in the configuration of the power system. Load disturbances, on the other hand, are the small random fluctuations in load demands. The system configuration usually remains unchanged after load disturbances. Recent trends toward full utilization of existing generation and transmission systems have increased the effects of these disturbances on power system security.

Power systems are planned and operated to withstand the occurrence of certain disturbances. The North American Electric Reliability Council defines security as the prevention of cascading outages when the bulk power supply is subjected to severe disturbances. The specific criteria which must be met are set by the individual reliability councils. Each council establishes the types of disturbances which the system must withstand without cascading outages. The following conditions, although conservative in nature, can ensure cascading outages will not occur: 1) when any of a specified set of disturbances occurs, the system will survive the ensuing transient and move into a steady-state condition, 2) no bus voltage magnitudes during transients are outside their permissible ranges, 3) in this new steady-state condition, no control devices, equipment or transmission lines are overloaded and no bus voltage magnitudes are outside their permissible ranges (say 5% of nominal). The first condition is related to the transient stability problem while the second one is related to the voltage-dip problem. The conditions are referred to as dynamic security. The third condition is referred to as static security.

Power system security analysis deals with the power system dynamic response to disturbances. In dynamic security analysis, the transition from the present operating condition to a new operating condition and the fact that

Manuscript received August 3, 1994; revised September 22, 1995. This work was supported in part by the National Science Foundation under Grant Numbers ECS-8957878 and ECS-95-05620, and in part from Electric Power Research Institute under Grant Number RP2473-61.

H.-D. Chiang and C.-C. Chu are with the School of Electrical Engineering, Cornell University, Ithaca, NY 14853 USA.

G. Cauley is with the Power Delivery Group, Electric Power Research Institute, Palo Alto, CA 94303 USA.

IEEE Log Number 9415903.

during the transient cascading outages will not be triggered are of concern. In static security analysis, the transition to a new operating condition is assumed, and the analysis is focused on the satisfaction of both operating and engineering constraints (overloading, voltage, etc.) The present-day power system operating environment has contributed to the increasing importance of the problems associated with dynamic security assessment of power systems. To a large extent, this is due to the fact that most of the major power system breakdowns are caused by problems relating to system dynamic responses [32] which mainly come from disturbances in power systems.

Maintaining power system dynamic security is a many-faceted problem in which thermal limits, transient stability, and voltage-dip issues must be addressed. In addition, adequate energy and capacity reserves must be available, and the frequency response of machine governors combined with the load characteristics must be such that frequency excursions are arrested within safe limits. This task is more complicated and difficult to accomplish due to the recent federally mandated open access to the transmission grids which is motivating providers of transmission services to strive to achieve higher loadings of transmission networks and facilities than ever before thought possible.

Transient stability analysis is concerned with a power system's ability to reach an acceptable steady-state (operating condition) following an event disturbance. The power system under this circumstance can be considered as going through changes in configuration in three stages: from prefault, to fault-on, and then to postfault systems. The prefault system is usually in a stable steady state. The fault occurs (e.g., a short circuit), and the system is then in the fault-on condition before it is cleared by the protective system operation. Stability analysis is the study of whether the postfault trajectory will converge (tend) to an acceptable steady-state as time passes.

Transient stability problems, which are the concern of this paper, have become a major operating constraint in specific regions of North America that rely on long distance transfers of bulk power, such as in most parts of the Western Interconnection and Hydro Quebec, and on interfaces between large supplies of hydro power in Canada and load areas to the south, such as in the Ontario/New York area and the Manitoba/Minnesota area. Transient stability problems have also been of concern to peninsular-type areas that are not as tightly connected to the rest of the network, such as the southern half of Florida. And there have been many individual generating facilities and localized areas with transient stability limitations under certain event disturbances. With increased numbers and volume of bulk power transfer, the trend now is for many more parts of the interconnected systems to become constrained by transient stability considerations. Transient stability will increasingly be a constraint to be evaluated in long distance transfers that result from transmission open access.

A major activity in utility system planning and operations is to test system transient stability relative to disturbances. Transient stability analysis programs are being used by power system planning and operating engineers to predict the response of the system to various disturbances. In these simulations, the behavior of a present or proposed power system is evaluated to determine its stability or its operating limits, or perhaps, to determine the need for additional facilities. Important conclusions and decisions are made based on the results of stability studies. It is therefore important to ensure that the results of stability studies are as timely and accurate as possible.

Until recently, transient stability analysis has been performed in power companies exclusively by means of numerical integrations to calculate generator behaviors relative to a given disturbance. By examining the behavior of the generators, one determines whether stability has been maintained or lost. This time-domain approach has several advantages: 1) it is directly applicable to any level of detail of power system models, 2) all the information of state variables during transient as well as steady-state is available, 3) simulation results can be directly interpreted by system operators. The chief disadvantages of this practice are: 1) it requires intensive time-consuming numerical integration, therefore it has not been suitable for on-line applications, 2) it does not provide information regarding the degree of stability (when the system is stable) and the degree of instability (when the system is unstable), 3) it does not provide information as to how to derive preventive control when the system is deemed unstable.

It is often desirable in practice to perform many power system stability studies to examine the effects of different fault locations and types, various operating conditions, different network topologies, and control device characteristics. For a typical large power system, thousands of nonlinear differential and algebraic equations must be solved, which takes tens of minutes of CPU time on a modern computer. This intensive computation requirement imposes severe constraints on the number of cases which can be studied. Moreover, the current power system operating environment motivates moving transient stability assessment from the off-line planning area into the on-line operating environment. There are significant benefits expected from this movement. First, one may be able to operate with margins reduced by a factor of 10 or more if the security assessment is based on actual system configuration and operating conditions, instead of assumed worst case conditions, as is done in off-line studies. As a simple example, a power transfer corridor whose actual stability boundary on a given hour can be computed to be 2500 MW could be forced to operate at a limit of 2000 MW based on the conservative assumptions inherent to off-line analysis. An on-line stability assessment using the actual system topology and real-time data could compute a limit of 2450 MW with enough certainty to allow the operator to load the system to that point. The savings realized in increased MW transaction capability can be $10 000 per hour. Another benefit of on-line analysis is that the amount of analysis can be reduced to those cases relevant to actual operating conditions, thereby freeing engineering resources for other critical activities. Thus there is always

Table 1 A Merit Comparison Between Direct Methods and the Time-Domain Approach

	Time-Domain Approach	Direct Methods (Based on Energy Functions)
Advantages	• applicable to general power system stability models • provide time responses of all state variables	• fast in computation • measure the degree of stability or instability • provide useful information regarding how to derive preventive control
Disadvantages	• slow in computation • no measure of degree of stability • no useful information regarding how to derive preventive control	• only applicable to power system stability models having energy functions • provide no time response of any state variables of the post-fault system

considerable incentive to find superior calculation methods for stability analysis.

An alternative approach to transient stability analysis employing energy functions, called direct methods, was originally proposed by Magnusson [49] in the late 1940's, and pursued in the 1950's by Aylett [9], and in the 1960's by Gless [38], and El-Abiad and Nagappan [30]. In contrast to the time-domain approach, direct methods determine system stability directly based on energy functions. These methods determine whether or not the system will remain stable once the fault is cleared by comparing the system energy (when the fault is cleared) to a critical energy value. Direct methods not only avoid the time-consuming solutions of step-by-step time-domain stability analysis of the postfault system, but also provide a quantitative measure of the degree of system stability. This additional information makes direct methods very attractive when the relative stability of different plans must be compared or when stability limits must be calculated quickly. Obviously a full step-by-step time-domain simulation cannot be run for each possible contingency. The operator needs to know not only if the system is safe in the present state, but also to what limits the system can be safely loaded to take advantage of, for example, economic opportunities. Direct methods can meet this need. A merit comparison between direct methods and the time-domain approach is summarized in Table 1.

Direct methods have a long development history spanning four decades, but until recently were thought by many to be impractical for large-scale power systems analysis with detailed models. However, recent developments have made direct methods a more practical means of solving large-scale power systems with network-preserving models. As seen in these early applications, direct methods provide several key advantages in performing on-line stability assessment using the actual power system configuration and on-line state estimated data. One key advantage is their ability to assess the degree of stability (or instability). The second advantage is their ability to calculate sensitivities of the stability margin to power system parameters, allowing for efficient computation of operating limits.

This paper starts with an intuitive understanding of direct methods and then develops energy function theory, followed by a theoretical foundation for direct methods for both network-reduction and network-preserving power system models. An advanced method, called the BCU method, of computing the controlling unstable equilibrium point (u.e.p.), which is essential in determining the critical energy value, is presented along with its theoretical foundation. In addition to an overview, new material is offered. Numerical solution algorithms capable of supporting on-line applications of direct methods are provided. These algorithms provide practical solutions to problems that have in the past made direct methods infeasible for on-line applications.

A major limitation of direct methods in the past has been the simplicity of the models used in various direct method implementations in software programs. Much of this limitation has been overcome and is presented in this paper. Another limitation has been that direct methods apply to first swing instability only. However, one of the most viable direct methods, the controlling u.e.p. method, is now shown in this paper to provide useful information for identifying multiswing unstable cases. In practical applications, the controlling u.e.p. method in conjunction with the BCU method, has shown promise as a tool for fast approximate contingency screening (thereby improving performance) and efficiently computing operating limits. This paper describes emerging applications of direct methods for on-line applications. Two examples include on-line transient stability assessments at the control center of Northern States Power Company and on-line transfer limit calculations at Ontario Hydro.

II. Mathematical Preliminaries

We next review some relevant concepts from nonlinear dynamical systems theory. To unify our notation, let

$$\dot{X}(t) = f(X(t)) \tag{1}$$

be the power system model under study, where the state vector $X(t)$ belongs to the Euclidean space R^n, and the function f: $R^n \rightarrow R^n$ satisfies the sufficient condition for the existence and uniqueness of solutions. The solution curve of (1) starting from X at $t = 0$ is called a (system) trajectory, denoted by $\Phi(x, \cdot)$: $R \rightarrow R^n$. Note that $\Phi(X, 0) = X$.

The concepts of *equilibrium point* (e.p.), *stable* and *unstable manifolds* are important in dynamical system theory. Each of these concepts is defined next. A detailed discussion of these concepts and their implications may be found in [39], [42], [60], [80], [81].

A state vector $\hat{X}$ is called an equilibrium point of system (1) if $f(\hat{X}) = 0$. We denote E to be the set of equilibrium points of the system. A state vector X is

called a *regular point* if it is not an equilibrium point. We say that an equilibrium point of (1) is *hyperbolic* if the Jacobian of $f(\cdot)$ at $\hat{X}$, denoted $J_f(X)$, has no eigenvalues with a zero real part. For a hyperbolic equilibrium point, it is a *(asymptotically) stable equilibrium point* if all the eigenvalues of its corresponding Jacobian have negative real parts; otherwise it is an *unstable equilibrium point*. If the Jacobian of the equilibrium point $\hat{X}$ has exactly one eigenvalue with positive real part, we call it a *type-one equilibrium point*. Likewise, $\hat{X}$ is called a *type-k equilibrium point* if its corresponding Jacobian has exactly k eigenvalues with positive real part. Throughout this section, it will be assumed that all the equilibrium points of system (1) are hyperbolic.

Let $\hat{X}$ be a hyperbolic equilibrium point. Its stable and unstable manifolds, $W^s(\hat{X})$ and $W^u(\hat{X})$, are defined as follows:

$$W^s(\hat{X}) := \{X \in R^n \colon \Phi(X,t) \to \hat{X} \text{ as } t \to \infty\}$$
$$W^u(\hat{X}) := \{X \in R^n \colon \Phi(X,t) \to \hat{X} \text{ as } t \to -\infty\}.$$

Both stable and unstable manifolds are invariant sets.[1]

For an asymptotically stable equilibrium point, it can be shown that there exists a number $\delta > 0$ such that $\|X_0 - \hat{X}\| < \delta$ implies $\Phi(X_0,t) \to \hat{X}$ as $t \to \infty$. If δ is arbitrarily large, then $\hat{X}$ is called a *global stable equilibrium point*. There are many physical systems containing stable equilibrium points but not global stable equilibrium points. A useful concept for these kinds of systems is that of *stability region* (also called *region of attraction*). The stability region of a stable equilibrium point X_s is defined as

$$A(X_s) := \{X \in R^n \colon \lim_{t\to\infty} \Phi(X,t) = X_s\}.$$

From a topological point of view, the stability region $A(X_s)$ is an open, invariant, and connected set. The boundary of stability region $A(X_s)$ is called the *stability boundary* (or *separatrix*) of X_s and will be denoted by $\partial A(X_s)$. The stability boundary is topologically an $(n-1)$-dimensional closed and invariant set.

A. Problem Formulation

The power system stability problem due to an event disturbance can be expressed in the following mathematical manner (see Fig. 1): In the prefault regime the system is at a known stable equilibrium point, say X_i. At some time t_f, the system undergoes a fault, termed the fault-on system, which results in a structural change in the system. Suppose the fault duration is confined to the time interval $[t_f, t_{cl}]$. During this interval, the system is governed by the fault-on dynamics described by

$$\dot{X}(t) = f_F(X(t)), \qquad t_f \le t < t_{cl} \tag{2}$$

where $X(t)$ is the vector of state variables of the system at time t. Sometimes, the fault-on system may involve more than one action from system relays and circuit breakers. In these cases, the fault-on system is described by several sets of equations:

$$\dot{X}(t) = f_F^1(X(t)), \qquad t_f \le t < t_{F,1}$$
$$\dot{X}(t) = f_F^2(X(t)), \qquad t_{F,1} \le t < t_{F,2}$$
$$\vdots$$
$$\dot{X}(t) = f_F^k(X(t)), \qquad t_{F,k} \le t < t_{cl}.$$

The number of the sets of equations corresponds to the number of actions due to the relays and circuit breakers. Each set of equations depicts the system dynamics due to one action from relays and circuit breakers. Suppose that the fault is cleared at time t_{cl} and the system, termed the postfault system, is henceforth governed by postfault dynamics described by

$$\dot{X}(t) = f(X(t)) \qquad t_{cl} \le t < \infty. \tag{3}$$

Next, assume that the postfault system (3) has an asymptotically stable equilibrium point X_s which satisfies operational constraints. The fundamental problem of transient stability is the following: starting from the postfault initial state $X(t_{cl})$, will the postfault system settle down to the steady state condition X_s? In other words, power system stability analysis is to determine whether the initial point of postfault trajectory is located inside the stability region (domain of attraction) of an acceptable stable equilibrium point (acceptable steady state).

The problem of direct stability analysis can be translated into the following: given a set of nonlinear equations with an initial condition, determine whether or not the ensuing trajectories will settle down to a desired steady-state without resorting to explicit numerical integrations. It is assumed in the area of direct methods that the following conditions are satisfied:

1) The prefault stable equilibrium point, X_s^{pre}, and the postfault equilibrium point, X_s, are sufficiently close to each other (so a nonlinear algebraic solver, such as the Newton method, with X_s^{pre} as the initial guess will find X_s) and

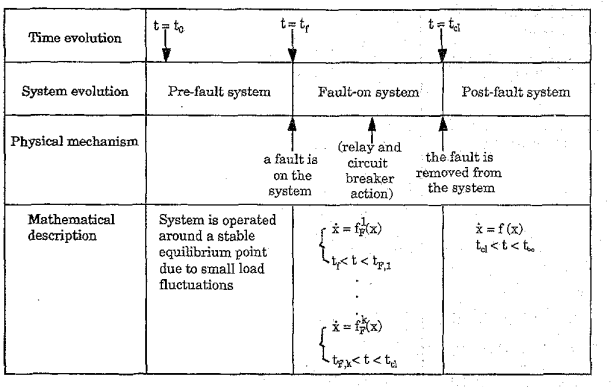

Fig. 1. The time evolution, system evolution, physical mechanism, and mathematical descriptions of the power system stability problem during the prefault, fault on, and postfault stages.

[1] A set $M \in R^n$ is called an *invariant set* of (1) if every trajectory of (1) starting in M remains in M for all t.

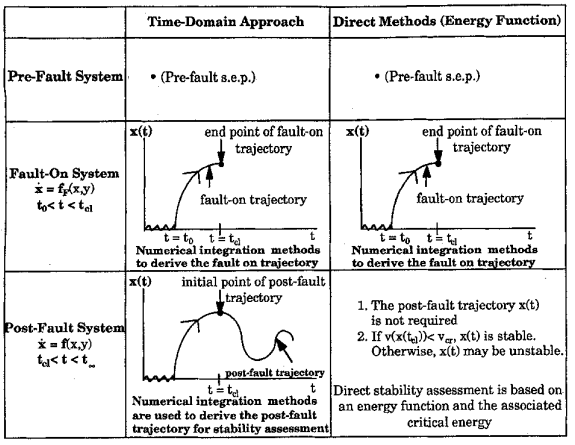

Fig. 2. Comparisons between time-domain approach and direct methods for power system transient stability problems.

2) the prefault stable equilibrium point, X_s^{pre}, lies inside the stability region of the postfault stable equilibrium point X_s.

Mathematical as well as physical arguments to support the above two assumptions can be found in [16].

As mentioned earlier, the most popular method of analyzing transient stability is to calculate the postfault behaviors via numerical integrations. On the other hand, direct methods first assume that the postfault system has a stable equilibrium point X_s which satisfies (power system) operational constraints (an acceptable steady state). Direct methods next determine, based on energy functions, whether the initial point of the postfault trajectory lies inside the stability region of the acceptable stable equilibrium point. If it does, direct methods then declare that the resulting postfault trajectory will converge to X_s without any information regarding the transients of the postfault trajectory. Comparisons between time-domain approach and direct methods for power system transient stability problems is summarized in Fig. 2. The basis of direct methods for the stability assessment of a postfault system is knowledge of the stability region: if the initial condition of the postfault system lies inside the stability region of a desired postfault stable equilibrium point, then one can ensure without performing any numerical integrations that the ensuing postfault trajectory will converge to the desired stable equilibrium point. Therefore, knowledge of the stability region plays an important role in direct methods. In the next section, a heuristic introduction of direct methods will be presented.

III. A Heuristic Introduction of Direct Methods

Heuristic arguments of the applicability of the direct methods can be derived from the classical equal area criterion. Consider one-machine-infinite-bus system described by the following equations:

$$\dot{\delta} = \omega$$
$$M\dot{\omega} = -D\omega - P_0 \sin\delta + P_m.$$

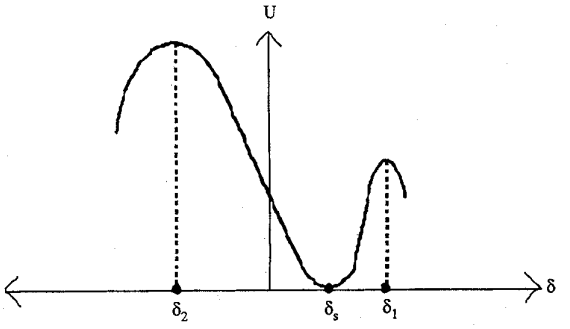

Fig. 3. The potential energy function $U(\delta)$ is a function of δ only and reaches its local maximum at the unstable e.p.'s δ_1 and δ_2.

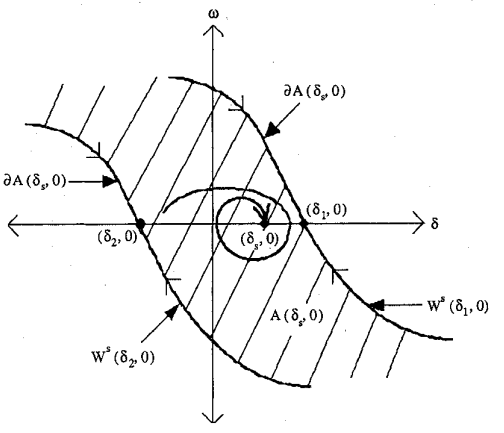

Fig. 4. The position of the stable equilibrium point $(\delta_s, 0)$ along with its stability $A(\delta_s, 0)$ (the shaded area). The stability boundary $\partial A(\delta_s, 0)$ is composed of the stable manifold of the u.e.p. $(\delta_1, 0)$ and the stable manifold of the u.e.p. $(\delta_2, 0)$.

There are three equilibrium points lying within the range of $\{(\delta, \omega) = -\pi < \delta < \pi, \omega = 0\}$, and they are $(\delta_s, 0) = (\arcsin(P_m/P_0), 0)$ which is a stable equilibrium point, and $(\delta_1, 0) = (\pi - \arcsin(P_m/P_0), 0), (\delta_2, 0) = (-\pi - \arcsin(P_m/P_0), 0)$ which are unstable equilibrium points. We consider the following function, termed energy function

$$E(\delta, \omega) = \tfrac{1}{2}M\omega^2 - P_m\delta - P_0 \cos\delta.$$

The energy function can be divided into kinetic energy $K(\omega)$ and potential energy functions $U(\omega)$,

$$E(\delta, \omega) = K(\omega) + U(\delta)$$

where $K(\omega) = \frac{1}{2}M\omega^2$ and $U(\delta) = -P_m\delta - P_0 \cos\delta$. The potential energy function $U(\cdot)$ as a function of δ is shown in Fig. 3. We notice that function $U(\delta)$ reaches its local maximum at the unstable e.p.'s δ_1 and δ_2.

The system is two-dimensional (2-D). Hence, the stability region of $(\delta_s, 0)$, shown in Fig. 4, is 2-D and the stability boundary $\partial A(\delta_s, 0)$ is composed of the stable manifold of the u.e.p. $(\delta_1, 0)$ and the stable manifold of the u.e.p.

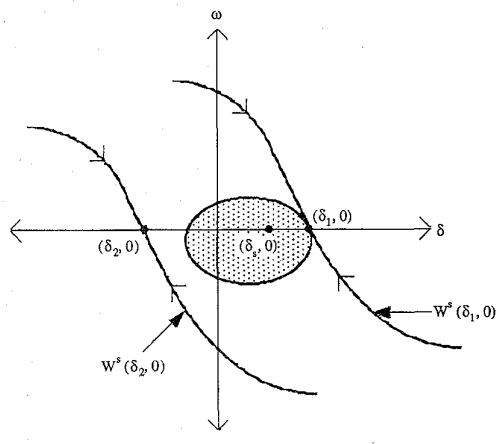

Fig. 5. The closest u.e.p. method uses the constant energy surface passing through the closest u.e.p. $(\delta_1, 0)$ to approximate the (entire) stability boundary $\partial A(\delta_s, 0)$. The shaded area is the estimated stability region by the closest u.e.p. method.

$(\delta_2, 0)$. The u.e.p. $(\delta_1, 0)$ has the lowest energy function value among all the u.e.p.'s on the stability boundary $\partial A(\delta_s, 0)$. Hence, $(\delta_1, 0)$ is termed the closest u.e.p. of $(\delta_s, 0)$ with respect to the energy function $U(\delta)$. We notice that:

1) The intersection between $A(\delta_s, 0)$ and the angle space $\{(\delta, \omega)\colon \delta = R, \omega = 0\}$ is $A_\delta := \{(\delta, \omega)\colon \delta \in [\delta_2, \delta_1], \omega = 0\}$.
2) The boundary of this one-dimensional region A_δ is composed of two points δ_1 and δ_2, where $(\delta_1, 0)$ and $(\delta_2, 0)$ are the u.e.p.'s on the stability boundary $\partial A(\delta_s, 0)$.
3) These two points δ_1 and δ_2 are characterized as being the local maxima of the potential energy function $U(\cdot)$.

The stability for this simple system can be directly assessed on the basis of the energy function $U(\delta)$: if a given postfault trajectory (δ, ω), after reaching a local maximum value of $U(\cdot), \delta$ starts to decrease, then the stability of this postfault trajectory is assured. The following two methods can be employed to assess the system's stability:

1) *Closest u.e.p. method:* This method uses the constant energy surface $\{(\delta, \omega)\colon V(\delta, \omega) = U(\delta_1)\}$ passing through the closest u.e.p. $(\delta_1, 0)$ to approximate the stability boundary $\partial A(\delta_s, 0)$. If a given state, say $(\delta_{cl}, \omega_{cl})$, whose energy function value $V(\delta_{cl}, \omega_{cl})$ is less than $U(\delta_1)$, then the state $(\delta_{cl}, \omega_{cl})$ is classified to be lying inside the stability region of $(\delta_s, 0)$ (see Fig. 5). Thus one can assert without numerical integration that the resulting trajectory will converge to $(\delta_s, 0)$. This method, termed the closest u.e.p. method, although simple, can give considerable conservative stability assessments; especially for those fault-on trajectories crossing the stability boundary $\partial A(\delta_s, 0)$ through $W^s(\delta_2, 0)$ (see Fig. 6(a)). For example, the postfault trajectory starting from the state P, which lies inside the stability region $A(\delta_s, 0)$, is classified to be unstable by the closest u.e.p. method while in fact the resulting trajectory will converge to $(\delta_s, 0)$ and hence it is stable (see Fig. 6(b)). We will elaborate on this problem of conservativeness later on.
2) *Controlling u.e.p. method:* This method aims to reduce the conservativeness of the closest u.e.p. method by taking the dependence of the fault-on trajectory into account. For those fault-on trajectories $(\delta(t), \omega(t))$ whose $\delta(t)$ component moves towards δ_1, the controlling u.e.p. method uses the constant energy surface passing through the u.e.p. $(\delta_1, 0)$ which is $\{(\delta, \omega)\colon E(\delta, \omega) = U(\delta_1)\}$ as the local approximation for the relevant stability boundary. In the same manner, for those fault-

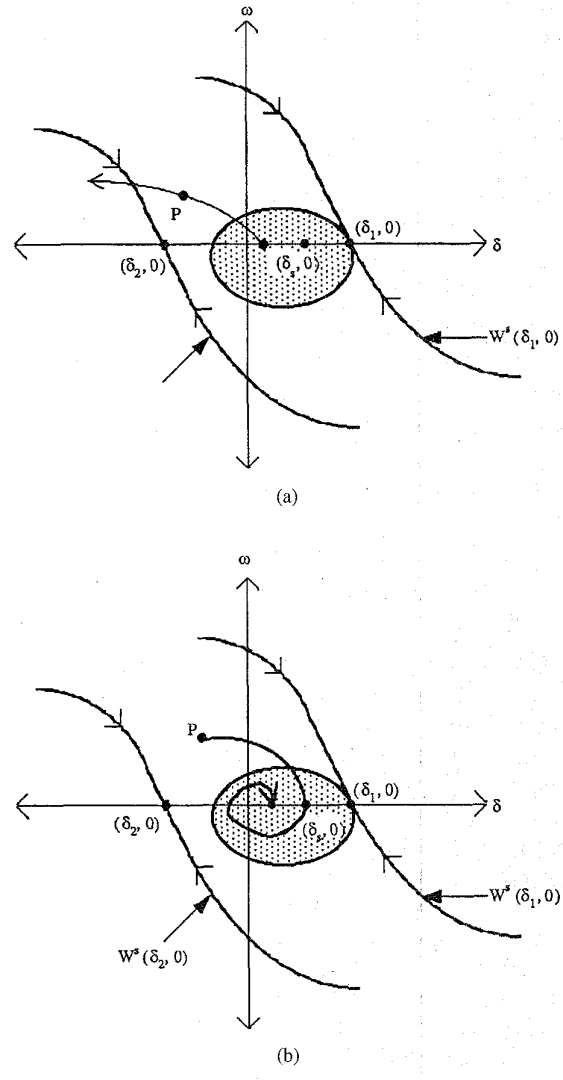

Fig. 6. (a) The closest u.e.p. method gives considerable conservative stability assessments for those fault-on trajectories crossing the stability boundary $\partial A(\delta_s, 0)$ through $W^s(\delta_2, 0))$. (b) The postfault trajectory starting from the state P, which lies inside the stability region $A(\delta_s, 0)$, is classified to be unstable by the closest u.e.p. method while in fact the resulting trajectory will converge to $(\delta_s, 0)$ and hence it is stable.

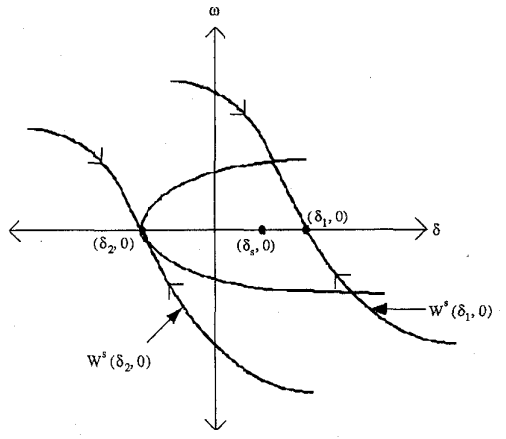

Fig. 7. *The controlling u.e.p. method uses the constant energy surface passing through the controlling u.e.p. to approximate the relevant stability boundary.*

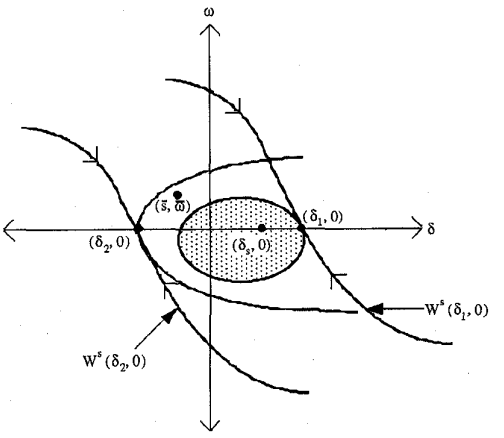

Fig. 8. The postfault trajectory starting from the state $(\bar{\delta}, \bar{\omega})$ which lies inside the stability region $A(\delta_s, 0)$ is classified to be stable by the controlling u.e.p. method while it is classified to be unstable by the closest u.e.p. method.

on trajectories $(\delta(t), \omega(t))$ whose $\delta(t)$ component moves towards δ_2, the constant energy surface passing through the u.e.p. $(\delta_2, 0)$, $\{(\delta, \omega)\colon E(\delta, \omega) = U(\delta_2)\}$ is chosen as the local approximation for the relevant stability boundary (see Fig. 7). Therefore, for each fault-on trajectory, there exists a unique corresponding unstable equilibrium point whose stable manifold constitutes the relevant stability boundary. The constant energy surface passing through the controlling u.e.p. can be used to accurately approximate the relevant part of the stability boundary toward which the fault-on trajectory is heading. If the energy function value of a given state is less than that of controlling u.e.p., then the state is classified to be lying inside the stability region of $(\delta_s, 0)$ by the controlling u.e.p. method. Thus one can assert without numerical integration that the resulting trajectory will converge to $(\delta_s, 0)$. This method, although more complex than the closest u.e.p. method, gives much more accurate and less conservative stability assessments than the closest u.e.p. method. For instance, the postfault trajectory starting from the state $(\bar{\delta}, \bar{\omega})$ which lies inside the stability region $A(\delta_s, 0)$ is correctly classified to be stable by the controlling u.e.p. method while it is classified to be unstable by the closest u.e.p. method (see Fig. 8). Again, this shows the conservativeness of the closest u.e.p. method which does not take the dependence of the fault-on trajectory in account.

The above exposition on the one-machine-infinite-bus system has outlined the key bases for both the closest u.e.p. method and the controlling u.e.p. method and highlighted their differences in stability assessment. The exposition also reveals the following three main steps needed for direct methods:

1) Constructing an energy function for the postfault system, say $V(\delta, \omega)$.
2) Computing the critical energy value V_{cr} for a given fault-on trajectory (say, based on the controlling u.e.p. method).
3) Comparing the energy value of the state when the fault is cleared, say $V(\delta_{cl}, \omega_{cl})$, with the critical energy value V_{cr}. If $V(\delta_{cl}, \omega_{cl}) < V_{cr}$, the postfault trajectory will be stable. Otherwise, it may be unstable.

To extend the above justification for direct methods to general multimachine power systems is nontrivial. This is partly due to the intrinsic difference between the nonlinear dynamics of 2-D systems and that of high-dimensional systems. We next present energy function theory for high-dimensional nonlinear systems and then apply the theory to develop a theoretical foundation for direct methods.

IV. Energy Function Theory

The basis of direct methods for the stability assessment of a postfault system is knowledge of the stability region: if the initial condition of the postfault system lies inside the stability region of a desired postfault stable equilibrium point, then one can ensure without performing any numerical integrations that the ensuing postfault trajectory will converge to the desired point. Therefore, knowledge of stability region plays an important role in direct methods.

This section reviews some analytical results associated with energy function theory which enable one to characterize limit sets, stability boundaries and stability regions. A more comprehensive development of energy function theory can be found in [15]. This section also shows how to use energy functions to estimate stability regions.

We say a function $V\colon R^n \mapsto R$ is an energy function for a system (1) if the following three conditions are satisfied:

1) the derivative of the energy function $V(X)$ along any system trajectory $X(t)$ is nonpositive, i.e., $\dot{V}(X(t)) \leq 0$.

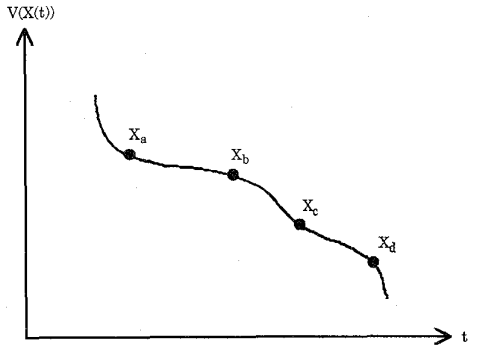

Fig. 9. Along the trajectory $X(t)$, the derivative of energy function is nonpositive and there are only countable points at which the derivative is zero. (for example, X_a, X_b, X_c, X_d).

2) If $X(t)$ is a nontrivial trajectory (i.e., $X(t)$ is not an equilibrium point (e.p.)), then along the nontrivial trajectory $X(t)$ the set $\{t \in R: \dot{V}(X(t)) = 0\}$has measure zero in R.
3) If a trajectory $X(t)$ has a bounded value of $V(X(t))$ for $t \in R^+$, then the trajectory $X(t)$ is also bounded. Stating this in brief:

$$\text{If } V(X(t)) \text{ is bounded, then } X(t) \text{ is also bounded.}$$

Property 1) indicates that the energy is nonincreasing along its trajectory, but does not imply that the energy is strictly decreasing along its trajectory. There may exist a time interval $[t_1, t_2]$ such that $\dot{V}(X(t)) = 0$ for $t \in [t_1, t_2]$. Properties 1) and 2) imply that the energy is strictly decreasing along any system trajectory. Property 3) states that along any system trajectory the energy function is a proper map[2] but its energy need not be a proper map for the entire state space (see Fig. 9). Obviously, an energy function is not a Lyapunov function.

In general, the behaviors of trajectories of general nonlinear dynamical systems could be very complicated, unless the underlying dynamical system has some special properties. For instance, every trajectory of system (1) having an energy function has only two modes of asymptotic behaviors: it either converges to an equilibrium point or goes to infinity (becomes unbounded) as time increases or decreases.

Theorem 4-1: [19], [23] (Global behavior of trajectories) If there exists a function satisfying conditions 1) and 2) of the energy function for system (1), then every bounded trajectory of system (1) converges to one of the equilibrium points.

Theorem 4-1 indicates that there does not exist any limit cycle (oscillation behavior) or bounded complicated behavior such as almost periodic trajectory, chaotic motion, etc. in the system. Applying this result to power system models, it indicates that for a power system model with an energy function, there is no complicated behavior such as chaotic motion and closed orbit (limit cycle). In Theorem 4-1 we have shown that the trajectory of system (1) either converges to one of the equilibrium points or goes to infinity. However, in the following, we will show that every trajectory on the stability boundary must converge to one of the equilibrium points on the stability boundary as time increases.

Theorem 4-2: [21] (The behavior of trajectories on the stability boundary). If there exists an energy function for system (1), then every trajectory on the stability boundary $\partial A(X_s)$ converges to one of the equilibrium points on the stability boundary $\partial A(X_s)$.

The significance of this theorem is that it offers a way to characterize the stability boundary. It asserts that the stability boundary $\partial A(X_s)$ is composed of several stable manifolds of the u.e.p.'s on the stability boundary.

Corollary 4-3: [19], [84] (Energy function and stability boundary). If there exists an energy function for system (1) which has an asymptotically stable equilibrium point X_s (but not globally asymptotically stable), then the stability boundary $\partial A(X_s)$ is contained in the set which is the union of the stable manifolds of the u.e.p.'s on the stability boundary $\partial A(X_s)$, i.e.,

$$\partial A(X_s) \subseteq \cup_{X_i \in \{E \cap \partial A(X_s)\}} W^s(X_i).$$

We next focus on how to estimate, via an energy function, the stability region of a high-dimension nonlinear system. We consider the following set

$$S_v(k) = \{X \in R^n: V(X) < k\} \tag{4}$$

where $V(\cdot)$: $R^n \to R$ is an energy function. Sometimes, we drop the subscript v of $S_v(k)$, simply writing $S(k)$, if it is clear from the context. We shall call the boundary of set (4),

$$\partial S(k) := \{X \in R^n: V(X) = k\}$$

the *level set* (or *constant energy surface*) and k the *level value*. If k is a regular value (i.e., $\nabla V(X) \neq 0$, for all $X \in V^{-1}(k)$), then by the Inverse Function Theorem $\partial S(k)$ is a C^r $(n-1)$-dimensional submanifold of R^n. Moreover, if $r > n-1$, then by the Morse–Sard theorem the set of regular values of V is residual; in other words, 'almost all' level values are regular. In particular, for almost all values of k, the level set $\partial S(k)$ is a C^r $(n-1)$-dimensional submanifold.

Generally speaking, this set $S(k)$ can be very complicated, with several different components even for the 2-D case. Let

$$S(k) = S^1(k) \cup S^2(k) \cup \cdots \cup S^m(k) \tag{5}$$

where $S^i(k) \cap S^j(k) = \phi$ when $i \neq j$. That is, each of these components is connected and disjoint from each other. Since $V(\cdot)$ is continuous, $S(k)$ is an open set. Because $S(k)$ is an open set, the level set $\partial S(k)$ is of $(n-1)$ dimensions. Furthermore, each component of $S(k)$ is an invariant set.

In spite of the possibility that a constant energy surface may contain several disjoint connected components, there is an interesting relationship between the constant energy surface and the stability boundary. This relationship is that

[2] We say that f: $X \to Y$ is a *proper map* if for each compact set D in Y, the set $F^{-1}(D)$ is compact in X.

at most one connected component of the constant energy surface $\partial S(r)$ has a nonempty intersection with the stability region $A(X_s)$ as shown in the following theorem.

Theorem 4-4: [15] (Constant energy surface and stability region)

Let X_s be a s.e.p. of the system (1) and $A(X_s)$ be its stability region. Then, the set $S(r)$ contains only one connected component which has a nonempty intersection with the stability region $A(X_s)$ if and only if $r > V(X_s)$.

Motivated by Theorem 4-4, we shall use the notation $S_{X_s}(r)$ to denote the connected set of $S(r)$ (whose level value is r) containing the stable equilibrium point X_s. In Fig. 10, the relation between the constant energy surfaces at different level values and the stability region $A(X_s)$ is shown. It is observed from this figure that the connected set S_{X_s} with a level value r smaller than the critical value is very conservative in the approximation of the stability boundary $\partial A(X_s)$. As the set S_{X_s} is expanded by increasing the level value r, the approximation gets better until this constant energy surface hits the stability boundary $\partial A(X_s)$ at some point. This point can be shown to be an u.e.p [20]. We call this point the *closest u.e.p.* of the s.e.p. X_s with respect to the energy function $V(\cdot)$. Furthermore, as we increase the level value r, the connected set S_{X_s} would contain points which lie outside the stability region $A(X_s)$. It is therefore inappropriate to approximate the stability boundary $\partial A(X_s)$ by the connected set S_{X_s} with a level value higher than that of the lowest point on the stability boundary $\partial A(X_s)$. From these figures, it becomes obvious that, among the several disjoint connected sets of the constant energy surface, the connected set S_{X_s} is the best candidate to approximate the stability boundary $\partial A(X_s)$. We remark that given a point in the state space (say, the initial point of the postfault system), it is generally difficult to determine which connected component of a level set contains the point. This is due to the fact that a level set usually contains several different components and they are not easy to differentiate based on an energy function value. Fortunately, the knowledge of a prefault stable equilibrium point, a fault-on trajectory and a postfault stable equilibrium point helps to identify the connected component of a level set that contains the initial point of postfault system.

The analytical results discussed in this section above will be extended in the next section to develop a theoretical foundation for the most viable direct method: the controlling u.e.p. method.

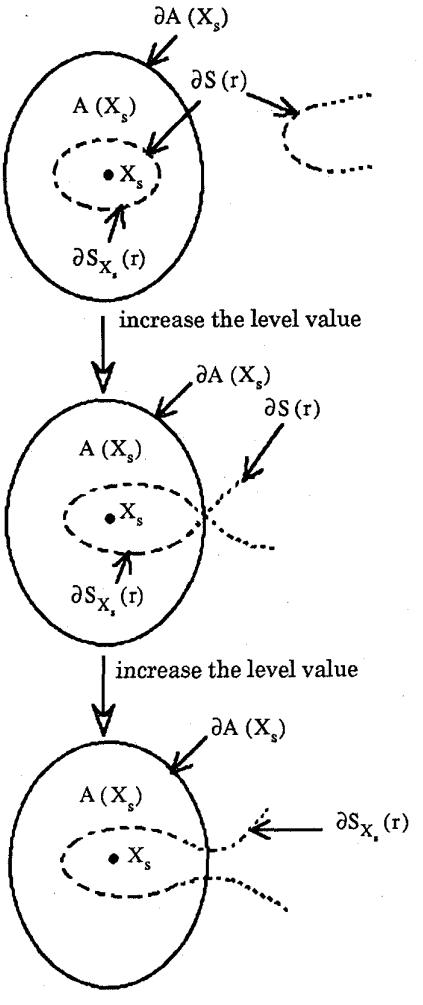

Fig. 10. The relation between the constant energy surfaces at different level values and the stability region $A(X_s)$.

V. The Controlling U.E.P. Method

From a nonlinear system viewpoint, transient stability analysis is essentially the problem of determining whether or not the fault-on trajectory at clearing time is lying inside the stability region of a desired stable equilibrium point of its postfault system. Hence, the main point in transient stability analysis is not to estimate the whole stability boundary of the postfault system. Instead, only the relevant part of the stability boundary toward which the fault-on trajectory is heading is of concern. When the closest u.e.p. method is applied to power system transient stability analysis, this method has been found to yield conservative results. In fact, in the context of transient stability analysis, the closest u.e.p. method provides an approximated stability boundary for the postfault system, and is independent of the fault-on trajectory. Thus the closest u.e.p. method can give very conservative results for transient stability analysis.

A desired method for determining the critical energy value would be the one which can provide the most accurate approximation of the part of the stability boundary toward which the fault-on trajectory is heading, even though it might provide a very poor estimate of the other part of stability boundary. To this end, the controlling u.e.p. method uses the constant energy surface passing through the controlling u.e.p. to approximate the part of stability boundary of the postfault system toward which the fault-on trajectory is heading. If, when the fault is cleared, the trajectory lies inside the energy surface passing through the controlling u.e.p., then the postfault system will be stable (i.e., the postfault trajectory will settle down to a stable operating point); otherwise, the postfault system may

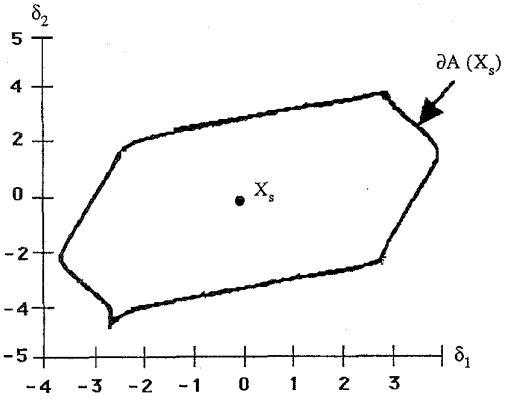

Fig. 11. The intersection between the stability boundary $\partial A(X_s)$ and the angle space (δ_1, δ_2).

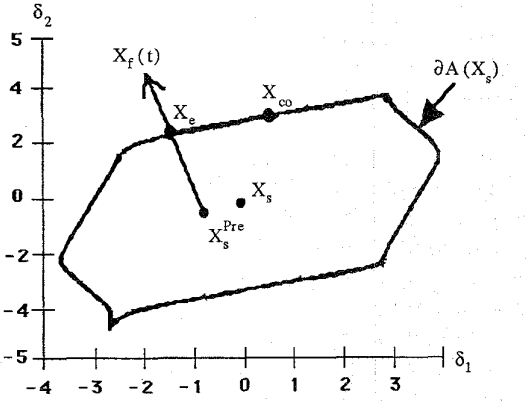

Fig. 12. The fault-on trajectory $X_f(t)$ leaves the stability boundary $\partial A(X_s)$ via passing through the stable manifold of the type-one e.p. X_{co} = (0.03333, 0, 3.10823, 0) at the exit point X_e.

be unstable. This is the essence of the controlling u.e.p. method.

A consensus seems to have emerged that among several methods for determining the critical energy value, the controlling u.e.p. method is the most viable for direct stability analysis of practical power systems [21], [15], [37], [57], [58]. The success of the controlling u.e.p. method, however, hinges upon its ability to find the correct controlling u.e.p. This section presents an overview and analysis of the controlling u.e.p. method. Section V-A uses a simple example to illustrate the concept of the controlling u.e.p. Section V-B studies the controlling u.e.p. method which is justified in Section V-C.

A. Concept

In order to illustrate the concept of the controlling u.e.p., we use the following simple numerical example, which closely represents a three-machine system, with machine number 3 as the reference machine.

$$\begin{aligned}\dot{\delta}_1 &= \omega_1 \\ \dot{\omega}_1 &= -\sin\delta_1 - 0.5\sin(\delta_1 - \delta_2) - 0.4\omega_1 \\ \dot{\delta}_2 &= \omega_2 \\ \dot{\omega}_2 &= -0.5\sin\delta_2 - 0.5\sin(\delta_2 - \delta_1) - 0.5\omega_2 + 0.05.\end{aligned} \tag{6}$$

It is easy to show that the following function is an energy function for this system.

$$\begin{aligned}V(\delta_1, \delta_2, \omega_1, \omega_2) = {} & \omega_1^2 + \omega_2^2 - 2\cos\delta_1 - \cos\delta_2 \\ & - \cos(\delta_1 - \delta_2) - 0.1\delta_2.\end{aligned} \tag{7}$$

Point $X^s = (\delta_1^s, \omega_1^s, \delta_2^s, \omega_2^s)$ = (0.02001, 0, 0.06003, 0), is a stable equilibrium point of the above postfault system. There are six type-one equilibrium points and six type-two equilibrium points on the stability boundary of X^s. Note that the unstable manifold of each of these equilibrium points converges to the s.e.p., X^s.

The stability boundary, $\partial A(X^s)$, is contained in the set which is the union of the stable manifolds of these six type-one e.p.'s and six type-two e.p.'s, as shown in Corollary 4-3. Fig. 11 shows numerically the intersection between the stability boundary $\partial A(X^s)$ and the angle space, (δ_1, δ_2).

For illustration purposes, we assume the fault-on trajectory, $X_f(t)$ due to a fault.[3]The fault-on trajectory, $X_f(t)$, leaves the stability boundary, $\partial A(X^s)$, via the stable manifold of the type-one e.p. X_{co} = (0.03333, 0, 3.10823, 0) at the exit point, X_e. X_{co} is termed the controlling u.e.p. relative to the fault-on trajectory $X_f(t)$. The time duration between p and X_e along the fault-on trajectory $X_f(t)$ is the so-called *critical clearing time*. If the fault is cleared before the fault-on trajectory reaches X_e, then the initial condition of the postfault trajectory lies inside the stability region $A(X_s)$; hence, the corresponding postfault trajectory will converge to X_s. Otherwise, the corresponding postfault trajectory will, as stated in Theorem 5-1, either converge to another stable equilibrium point[4] or diverge.[5]

In the operation or operational planning environment, calculating the critical clearing time relative to a fault is not practical because the reclosure times of protective relays in the system are already set. The key concern under this circumstance is whether, after the fault is cleared, the system will remain stable or not. This is explained as follows: Given a prefault stable equilibrium point X_s^{pre} and a fault-on trajectory $X_f(t)$ with a preset fault clearing time, let X_{cl} be the corresponding initial point of the postfault trajectory and $W^s(X_{co})$ be the stable manifold of the corresponding controlling u.e.p. X_{co}. The task of determining, based on the stable manifold $W^s(X_{co})$, whether the segment of the

[3]The fault-on trajectory $X_f(t)$ in practice has nonzero components of ω.

[4]Physically, this implies a pole-slip phenomenon.

[5]The corresponding trajectory becomes unbounded; of course power system protective devices will be activated and the underlying model becomes invalid.

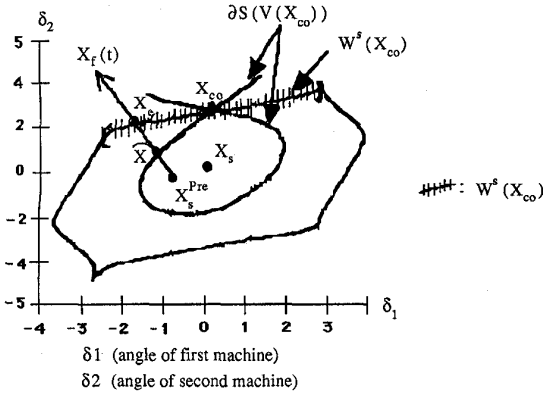

Fig. 13. Numerical relationship between the stable manifold $W^s(X_{co})$, the stability boundary and the constant energy surface passing through X_{co}.

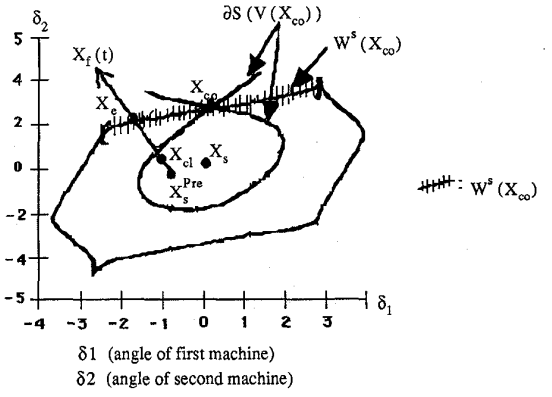

Fig. 14. The intersection between the stability boundary $\partial A(X_s)$ and the angle space (δ_1, δ_2).

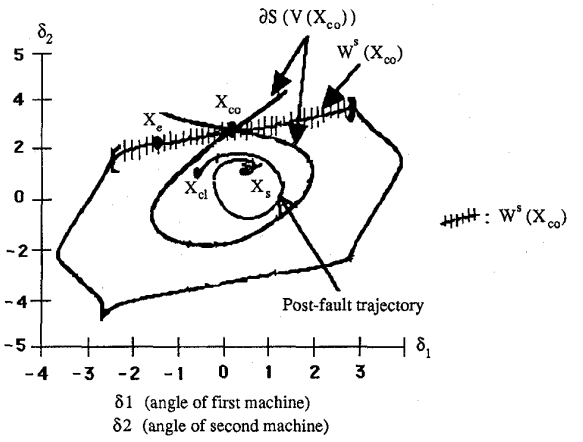

Fig. 15. The postfault trajectory starting from X_{cl} will settle down to X_s because X_{cl} lies inside the stability region $A(X_s)$.

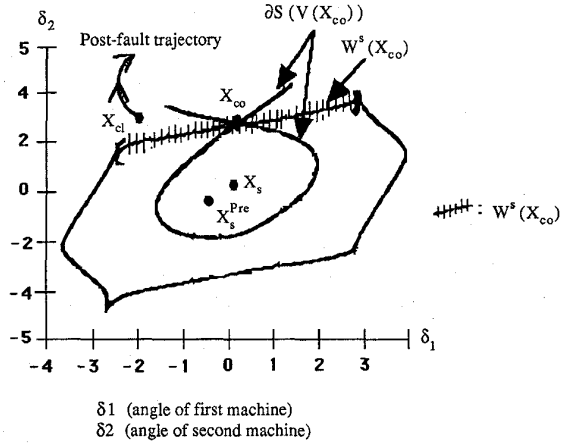

Fig. 16. X_{cl} lies outside the stability region $A(X_s)$, in which we have $V(X_{co}) < V(X_e) < V(X_{cl})$ and the postfault trajectory starting from X_{cl} will not settle down to X_s.

fault-on trajectory, $X_f(t)$, from X_s^{pre} to X_{cl} lies inside the stability region $A(X_s)$ is numerically very difficult, if not impossible. The main reason for this difficulty is due to the lack of an explicit expression for stable manifolds. However, the task is relatively easy if an energy function instead of the stable manifold $W^s(X_{co})$ is given. To elaborate on this point, let us go back to the previous numerical example and examine Fig. 13, which shows the relationship between the stable manifold $W^s(X_{co})$ and the constant energy surface passing through X_{co}. In order for the fault-on trajectory $X_f(t)$ to pass through the constant energy surface $\partial S(V(X_{co}))$, the point X_{cl} must have an energy value greater than the energy value at the controlling u.e.p. X_{co}; i.e., $V(X_{cl}) > V(X_{co})$. Hence, the task of determining whether the segment of the fault-on trajectory $X_f(t)$ from X_s^{pre} to X_{cl} lies inside the stability region $A(X_s)$ boils down to the task of comparing two scalars: $V(X_{cl})$ and $V(X_{co})$. If $V(X_{cl}) \leq V(X_{co})$, then the controlling u.e.p. method asserts that X_{cl} lies inside the stability region. Indeed, the segment of the fault-on trajectory $X_f(t)$ from X_s^{pre} to X_{cl} lies inside the stability region $A(X_s)$ (see Fig. 14). In this case, the postfault trajectory starting from X_{cI} will converge to the stable equilibrium point X_s (see Fig. 15).

On the other hand, if $V(X_{cl}) > V(X_{co})$, the controlling u.e.p. method asserts that X_{cl} lies outside the stability region; however, the segment X_s^{pre} to X_{cl} may not lie totally inside the stability region $A(X_s)$. Two cases are possible. In the first case, X_{cl} lies outside the stability region $A(X_s)$, in which we have $V(X_{co}) < V(X_e) < V(X_{cl})$ and the postfault trajectory starting from X_{cl} will not converge to X_s (see Fig. 16). In the second case, X_{cl} still lies inside the stability region $A(X_s)$, in which we have $V(X_{co}) < V(X_{cl}) < V(X_e)$ and the postfault trajectory starting from X_{cl} will still converge to X_s (see Fig. 17). The second case points out the slight conservative nature of the controlling u.e.p. method in estimating the relevant stability region and the stability property of the postfault trajectory. The above reasoning forms the basis of the energy function based controlling u.e.p. method which will be theoretically justified later in this section.

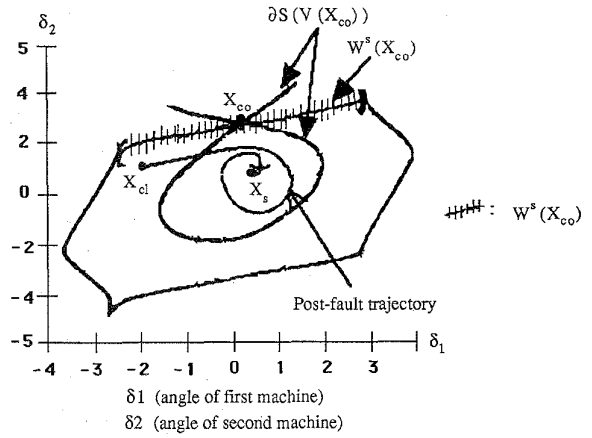

Fig. 17. X_{cl} still lies inside the stability region $A(X_s)$, in which we have $V(X_{co}) < V(X_{cl}) < V(X_e)$ and the postfault trajectory starting from X_{cl} will still settle down to X_s.

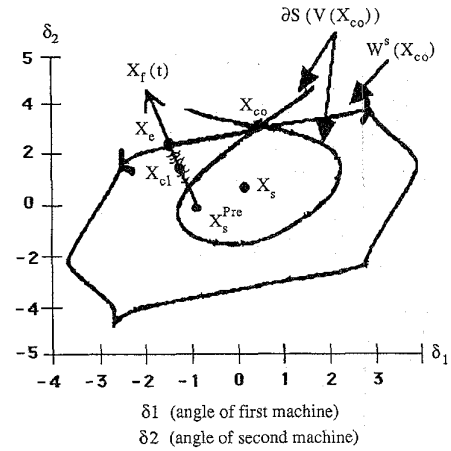

Fig. 18. When a fault is cleared at the portion highlighted in this figure in which case $V(X_e) > V(X_{cl}) > V(X_{co})$, the controlling u.e.p. method will predict a stable postfault trajectory to be unstable. This is the only scenario in which the controlling u.e.p. method gives conservative stability predictions.

The above analysis points out that the controlling u.e.p. method will:

Case 1: predict a stable postfault trajectory, either first-swing or multiswing, to be stable, in which case $V(X_{cl}) < V(X_{co})$ (cf. Fig. 14); or

Case 2: predict an unstable postfault trajectory, either first-swing or multiswing, to be unstable, in which case $V(X_{cl}) > V(X_{co})$ (cf. Fig. 16); or

Case 3: predict a stable postfault trajectory, either first-swing or multiswing, to be unstable, in which case $V(X_e) > V(X_{cl}) > V(X_{co})$, which is the only scenario in which the controlling u.e.p. method gives conservative predictions (see Fig. 18).

The controlling u.e.p. method always classifies unstable trajectories to be unstable (see case 2). This nice property of the controlling u.e.p. method distinguishes the method itself from other methods. Depending on the characteristics of the fault-on trajectory and the property of the energy function, the controlling u.e.p. method may classify stable trajectories to be stable (see Case 1) or may classify stable trajectories to be unstable (see Case 3). The conservative nature shown in Case 3 is not surprising because the energy function, on which the controlling u.e.p. method is based, maps the state space (which is n-dimensional) into a scalar (which is 1D). Since this map is not one-to-one,[6] the conservative nature of the controlling u.e.p. method is expected.

B. The Controlling U.E.P. Method

The controlling u.e.p. method for direct stability analysis of large-scale power systems proceeds as follows:

1) Determination of the Critical Energy

Step 1.1: Find the controlling u.e.p., X_{co}, for a given fault-on trajectory $X_f(t)$.

Step 1.2: The critical energy, v_{cr}, is the value of energy function $V(\cdot)$ at the controlling u.e.p., i.e.,

$$v_{cr} = V(X_{co})$$

[6]It maps all the points in the state space with the same energy into one scalar.

2) Determination of Stability

Step 2.1: Calculate the value of the energy function $V(\cdot)$ at the time of fault clearance (say at time t_{cl})

$$v_f = V(X_f(t_{cl})).$$

Step 2.2: If $v_f < v_{cr}$, then the postfault system is stable. Otherwise, it may be unstable.

The controlling u.e.p. method can be viewed as a method which yields an approximation of the relevant part of the stability boundary of the postfault system to which the fault-on trajectory is heading. It uses the connected constant energy surface passing through the controlling u.e.p. to approximate the relevant part of stability boundary.

C. Analysis of the Controlling U.E.P. Method

Theorem 5-1 below, which is a slight extension of that in [16], gives a rigorous justification of the controlling u.e.p. method. We will use the notation $(\overline{A}(X_s))^c$ to stand for the complement of the closure of the stability region $A(X_s)$.

Theorem 5-1: (Fundamental theorem for the controlling u.e.p. method) Consider a general nonlinear system described by system (1) which has an energy function $V(\cdot)$: $R^n \to R$. Let X_{co} be an equilibrium point on the stability boundary $\partial A(X_s)$ of this system. Let $r > V(X_s)$ and

- $S(r)$:= the connected component of the set $\{X\colon V(X) < r\}$ containing X_s, and
- $\partial S(r)$:= the connected component of the set $\{X\colon V(X) = r\}$ containing X_s.

Then:

1) The connected constant energy surface $\partial S(V(X_{co}))$ intersects with the stable manifold $W^s(X_{co})$ only at point X_{co}; moreover, the set $S(V(X_{co}))$ has an empty intersection with the stable manifold $W^s(X_{co})$. In

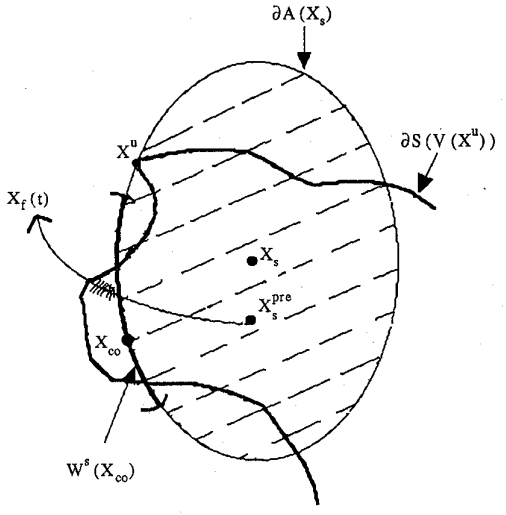

Fig. 19. Although set $S(V(X^u))$ contains only part of the stable manifold $W^s(X_{co})$, the fault-on trajectory $X_f(t)$ passes through the connected constant energy surface $\partial S(V(X^u))$ before it passes through the stable manifold $W^s(X_{co})$. In this situation, the controlling u.e.p. method using X^u as the controlling u.e.p. gives an inaccurate stability assessment when the postfault trajectory starts from the portion highlighted.

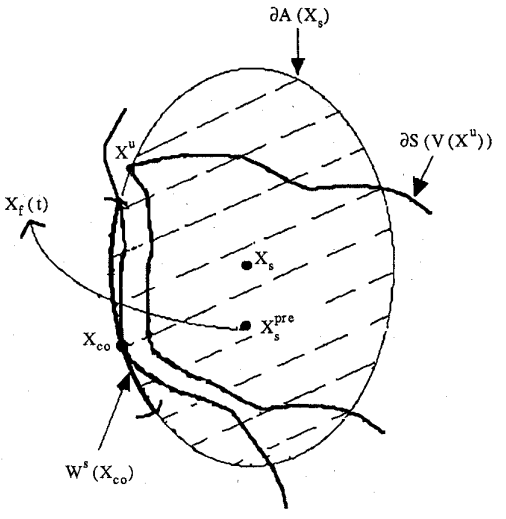

Fig. 20. Set $S(V(X^u))$ has an empty intersection with the stable manifold $W^s(X_{co})$ and the fault-on trajectory $X_f(t)$ passes through the connected constant energy surface $\partial S(V(X^u))$ before it passes through the connected constant energy surface $\partial S(V(X_{co}))$. In this situation, the controlling u.e.p. method using X_u as the controlling u.e.p. always gives more conservative stability assessment than that of using the controlling u.e.p. X_{co}.

other words, $\partial S(V(X_{co})) \cap W^s(X_{co}) = X_{co}$ and $S(V(X_{co})) \cap W^s(X_{co}) = \phi$.

2) $S(V(X_u)) \cap W^s(X_{co}) \neq \phi$ if X_u is an e.p. and $V(X_u) > V(X_{co})$.
3) $S(V(X_u)) \cap W^s(X_{co}) = \phi$ if X_u is an e.p. and $V(X_{co}) > V(X_u)$.
4) If X_{co} is not the closest u.e.p., then $\partial S(V(X_{co})) \cap (\overline{A}(X_s))^c \neq \phi$.
5) Any connected path starting from a point $P \in \{\partial S(V(X_{co})) \cap A(X_s)\}$ and passing through the stable manifold $W^s(X_{co})$ must hit the set $\partial S(V(X_{co}))$ first before it hits $W^s(X_{co})$.

Parts 1 and 5 of Theorem 5-1 implies that, for any fault-on trajectory $X_f(t)$ starting from a point $X_s^{\text{pre}} \in A(X_s)$ and $V(X_s^{\text{pre}}) < V(X_{co})$, if the exit point of this fault-on trajectory $X_f(t)$ lies on the stable manifold of X_{co}, this fault-on trajectory $X_f(t)$ must pass through the connected constant energy surface $\partial S(V(X_{co}))$ before it passes through the stable manifold of X_{co} (thus exiting the stability boundary $\partial A(X_s)$). Therefore, the connected constant energy surface $\partial S(V(X_{co}))$ can be used to approximate the relevant part of the stability boundary $\partial A(X_s)$ for the fault-on trajectory $X_f(t)$. Parts (1) and (5) of Theorem 5-1 also show the slight conservative nature of the controlling u.e.p. method in direct stability assessment. More importantly, the controlling u.e.p. method can directly detect both first swing and multiswing instabilities; although historically other direct methods have been said to be only applicable to first-swing stability analysis.

On the other hand, parts (2) and (4) of Theorem 5-1 state that the following two situations may occur:

Case 1: Set $S(V(X^u))$ contains only part of the stable manifold $W^s(X_{co})$.

Case 2: Set $S(V(X^u))$ contains the whole stable manifold $W^s(X_{co})$.

In case 1, the fault-on trajectory $X_f(t)$ may pass through the connected constant energy surface $\partial S(V(X^u))$ before it passes through the stable manifold $W^s(X_{co})$. In this situation, the controlling u.e.p. method using X^u as the controlling u.e.p. still gives an accurate stability assessment. Yet the fault-on trajectory $X_f(t)$ may pass through the connected constant energy surface $\partial S(V(X^u))$ after it passes through the stable manifold $W^s(X_{co})$ (see Fig. 19). In this situation, the controlling u.e.p. method using X^u as the controlling u.e.p. gives an inaccurate stability assessment. In particular, it may classify a postfault trajectory (when the fault is cleared at the portion highlighted in Fig. 19) to be stable when in fact it is unstable. This is a very undesirable classification.

In case 2, the fault-on trajectory $X_f(t)$ always passes through the connected constant energy surface $\partial S(V(X^u))$ after it passes through stable manifold $W^s(X_{co})$. Under this situation, the controlling u.e.p. method using X_u as the controlling u.e.p. always gives an inaccurate stability assessment. Again, it classifies the postfault trajectory (when the fault is cleared at the portion highlighted in Fig. 19) to be stable when in fact it is unstable.

Parts [3] and [4] of Theorem 5-1 assert that the set $S(V(X^u))$ has an empty intersection with the stable manifold $W^s(X_{co})$. Under this situation, the fault-on trajectory $X_f(t)$ always passes through the connected constant energy surface $\partial S(V(X^u))$ first before it passes through the connected constant energy surface $\partial S(V(X_{co}))$ (see Fig. 20). Thus using $V(X_u)$ as the critical energy value always gives even more conservative stability assessments than using that of the exact controlling u.e.p., X_{co}.

From the above analysis, it is clear that for a given fault-on trajectory $X_f(t)$, if the exit point of $X_f(t)$ lies on the stable manifold of an u.e.p. X_{co}, then using other u.e.p.'s instead of using X_{co} as the controlling u.e.p., can give an incorrect stability assessment in both directions: either too conservative or optimistic (i.e., classifying an unstable trajectory as stable).

In summary, the task of finding the precise controlling u.e.p. of a fault-on trajectory is essential for direct transient stability analysis. Using the energy value of a wrong controlling u.e.p. as a critical value is likely to give inaccurate stability assessment. Unfortunately, the task of finding the exact controlling u.e.p. of a given fault for general power system models is very difficult because:

- The controlling u.e.p. is a particular u.e.p. embedded in a large-degree state-space.
- The controlling u.e.p. is the first u.e.p. whose stable manifold is hit by the fault-on trajectory (at the exit point).
- The exit point is very difficult to detect.

A method which can find the controlling u.e.p. relative to any given fault has been presented in [16]. This method is based on the time-domain simulation approach; hence it is slow in nature. The role of this time-domain method is only to serve as a bench-mark to check the correctness of the controlling u.e.p. obtained by direct methods. It may prove fruitful to develop a tailored solution algorithm for finding controlling u.e.p.'s. by exploiting special properties as well as some physical and mathematical insights of the underlying power system model. In later sections, we will detail such a systematic method for finding controlling u.e.p.'s for both network-reduction and network-preserving power system models.

VI. Direct Methods for Network-Reduction Power System Models

Traditionally, direct methods have been based on the network-reduction model where all the load representations are expressed in constant impedance and the entire network representation is reduced to the generator internal buses. In this section we discuss direct methods for network-reduction power system models.

A. Network-Reduction Models

1) The Classical Model: We review the network reduction with the classical generator model for transient stability analysis. Consider a power system consisting of n generators. Let the loads be modeled as constant impedances. The dynamics of the ith generator can be represented, using the angles of the infinite bus as a reference, by the following equations [6]:

$$\begin{aligned} \dot{\delta}_i &= \omega_i \\ M_i\dot{\omega}_i &= -D_i\omega_i + P_{m_i} - P_{e_i}, \qquad i = 1, \cdots, n \end{aligned} \tag{8}$$

where

$$P_{e_i} = \sum_{j\neq i}^{n+1} V_iV_jB_{ij}\sin(\delta_i - \delta_j) + \sum_{j\neq i}^{n+1} V_iV_jG_{ij}\cos(\delta_i - \delta_j)$$

V_i is the constant voltage behind direct axis transient reactance. M_i is the generator's moment of inertia. D_i is the generator's damping constant. B_{ij} and G_{ij} terms represent the transfer susceptance and conductance of the (i,j) element in the reduced admittance matrix of the system, respectively. P_{m_i} is the mechanic power.

2) The One-Axis Generator Model with Exciters: This model includes one circuit for the field winding of the rotor, i.e., this model considers the effects of field flux decay. As a result, the voltage behind the direct transient reactance is no longer a constant. Sasaki first included such models for direct stability analysis [69]. The dynamics of each generator are then described by the following equations:

$$\begin{aligned} \dot{\delta}_i &= \omega_i \\ M_i\dot{\omega}_i &= -D_i\dot{\delta}_i + P_{mi} \\ &\quad - \sum_{j=1,i\neq j}^{n} V_iV_j(B_{ij}\sin\delta_{ij} + G_{ij}\cos\delta_{ij}) \\ \frac{T'_{doi}}{x_{di}-x'_{di}}\dot{V}_i &= \frac{1}{x_{di}-x'_{di}}E_{f\,di} - \frac{1-(x_{di}-x'_{di})B_{ii}}{x_{di}-x'_{di}}V_i \\ &\quad + \sum_{j=1,i\neq j}^{n} V_j(B_{ij}\cos\delta_{ij} + G_{ij}\sin\delta_{ij}). \end{aligned} \tag{9}$$

3) The One-Axis Generator Plus First Order AVR Model: When the exciter control action is included in the generator model, at least one additional differential equation is needed to account for it:

$$T_{vi}\dot{E}_{fdi} = -E_{fdi} - \mu_iV_{ti} + l_i.$$

We assume the terminal voltage V_{ti} of each generator has a linear relationship with its quadrature component V_{tqi}, i.e., $V_{ti} = k_iV_{tqi}$, where k_i is a positive constant. Thus using the relationship $V_{tqi} = x'_{di}I_{di} + V_i$, the complete dynamics can be simplified as [51]

$$\begin{aligned} \dot{\delta}_i &= \omega_i \\ M_i\dot{\omega}_i &= -D_i\dot{\delta}_i + P_{mi} \\ &\quad - \sum_{j=1,i\neq j}^{n} V_iV_j(B_{ij}\sin\delta_{ij} + G_{ij}\cos\delta_{ij}) \\ \gamma_i\dot{V}_i &= -\alpha_iV_i + \beta_iE_{fdi} \\ &\quad + \sum_{j=1,i\neq j}^{n} V_j(B_{ij}\cos\delta_{ij} + G_{ij}\sin\delta_{ij}) \\ \xi_i\dot{E}_{fdi} &= -\eta_iV_i - \phi_iE_{fdi} \\ &\quad - \sum_{j=1,i\neq j}^{n} V_j(B_{ij}\cos\delta_{ij} + G_{ij}\sin\delta_{ij}) + l_i \end{aligned} \tag{10}$$

where

$$\begin{aligned} \alpha_i &= -B_{ii} + \frac{1}{x_{di}} - x'_{di}, & \beta_i &= \frac{1}{x_{di}} - x'_{di}, \\ \gamma_i &= \frac{T'_{doi}}{x_{di}} - x'_{di}, & \eta_i &= B_{ii} + \frac{1}{x'_{di}}, \\ \phi_i &= \frac{1}{\mu_ik_ix'_{di}}, & \xi_i &= \frac{T_{vi}}{\mu_ik_ix'_{di}} \end{aligned}$$

are constants. Here we follow the IEEE recommended notation [58], which is somewhat different from the original paper [51] in which the industry notation is used.

4) The Two-Axis Generator Model with Exciters: For generators with the *salient-pole* case, due to the armature reaction flux alignment effect, the internal voltage dynamics is decomposed into two perpendicular parts with different time constants: direct-axis voltage E'_{di} and quadrature-axis voltage E'_{qi}. Using the angle of the infinite bus as a reference, the dynamics of the ith generator modeled by the two-axis machine model with a simplified first-order exciter model can be represented by the following equations [37], [58], [64].

$$\begin{aligned}
\dot{\delta}_i &= \omega_i \\
M_i\dot{\omega}_i &= P_{m_i} - E'_{di}I_{di} - E'_{qi}I_{qi} + (x'_{qi} - x'_{di})I_{di}I_{qi} \\
T'_{doi}\dot{E}'_{qi} &= E_{FDi} - E'_{qi} + (x_{di} - x'_{di})I_{di} \\
T'_{qoi}\dot{E}'_{di} &= -E'_{di} - (x_{qi} - x'_{qi})I_{qi} \\
T'_{vi}\dot{E}'_{fdi} &= -E'_{fdi} + K_{Ai}(V_{\text{ref}} - V_{ti}).
\end{aligned} \tag{11}$$

B. Exact and Numerical Energy Functions

We next discuss a procedure to construct energy functions for the above four network-reduction power system models.

If the transfer conductance of the reduced network is zero (i.e., $G_{ij} = 0$), then the above four models, except for the two-axis generator model with exciters, can be written in the following compact form:

$$\begin{aligned}
T\dot{x} &= -\frac{\partial}{\partial x}U(x,y) \\
\dot{y} &= z \\
M\dot{z} &= -Dz - \frac{\partial}{\partial y}U(x,y)
\end{aligned} \tag{12}$$

where T, M, and D are positive diagonal matrices. Consider the function

$$W(x,y,z) = K(z) + U(x,y) = \tfrac{1}{2}z^T M z + U(x,y)$$

we show that $W(x,y,z)$ is an energy function for system (12). Differentiating $W(x,y,z)$ along the system trajectory gives

$$\begin{aligned}
\dot{W}(x(t),y(t),z(t)) &= \frac{\partial W^T}{\partial x}\dot{x} + \frac{\partial W^T}{\partial y}\dot{y} + \frac{\partial W^T}{\partial z}\dot{z} \\
&= -\frac{\partial U^T}{\partial x}T^{-1}\frac{\partial U}{\partial x} - z^T D z \le 0.
\end{aligned}$$

This inequality shows that condition (1) of the energy function is satisfied. Suppose that there is an interval $t \in [t_1, t_2]$ such that $\dot{W}(x(t),y(t),z(t)) = 0$. From (12) and (13), we have $z(t) = 0$ and $\dot{x}(t) = 0$ for $t \in [t_1, t_2]$, which implies that $y(t)$ is a constant for $t \in [t_1, t_2]$. It then follows from (12) that the system state is at an equilibrium point, hence condition (2) of the energy function also holds.

The task of verifying condition (3) of the energy function (i.e., energy function is a dynamic proper map) is the most involved. It often requires exploring the special structure of the underlying model. This condition has been verified for the classical generator model in [21]. For the other network-reduction models, we will first prove that along every trajectory with bounded energy $W(x,y,z), x(t)$ is also bounded. We will then show that $y(t)$ and $z(t)$ are also bounded. For purpose of illustration, we will only prove the case for the one-axis generator model. In this model, the internal voltage dynamics can be put into the following compact form [25]:

$$T\dot{V} = \overline{A}(\delta(t))V + E_{fd}$$

where

$$\begin{aligned}
&T_{ii} = T'_{doi}, \quad T_{ij} = 0, \qquad i \neq j, \quad \overline{A}(\delta(t)) = MN - I, \\
&M_{ii} = x_{di} - x'_{di}, \quad M_{ij} = 0, \qquad i \neq j, \quad \text{and} \\
&N_{ij} = B_{ij}\cos\delta_{ij}.
\end{aligned}$$

Since along any nontrivial trajectory with a bounded energy, the set $\Gamma = \{t \in R^+ : \det\overline{A}(\delta(t)) = 0\}$ has measure zero and $\dot{V}(t)$ is bounded, it follows that $V(t) = \overline{A}(\delta(t))^{-1}(T\dot{V} - E_{fd})$ is also bounded. Since $V(t)$ is bounded, it follows from Theorem 3.3 in [22] that $\delta(t)$ and $\omega(t)$ are also bounded.

For the above various network-reduction models, the corresponding variables x, y, z and the potential energy functions $U(x,y)$ can be found in [25]. Note that these energy functions can be decomposed into a sum of two separable functions: kinetic energy, which is related to the variable z only, and potential energy function, which is related to the variables x and y. This observation will prove useful in our sequel analysis.

To derive an energy function for network-reduction models with nonzero transfer conductance of the reduced Y-bus matrix is a challenging task. Considerable efforts have been made to find energy functions for these models [13], [14], [40], [48], [53]. Unfortunately, these efforts, either based on the classical Lure–Postnikov-type Lyapunov function approach or the first integral approach, have been in vain. Narasimhamurthi has shown that attempts to accommodate line losses by a smooth transformation of the energy functions for power systems without losses do not lead to a local Lyapunov function [53]. It has been shown that there does not exist a general form of 'exact' energy function for power systems with transfer conductances [14]. However, global energy functions still exist for certain network-reduction power system models under certain moderate conditions [24].

A compact representation of the above four network-reduction models with transfer conductance is

$$\begin{aligned}
T\dot{x} &= -\frac{\partial}{\partial x}U(x,y) + g_1(x,y) \\
\dot{y} &= z \\
M\dot{z} &= -Dz - \frac{\partial}{\partial y}U(x,y) + g_2(x,y)
\end{aligned} \tag{13}$$

where $g_1(x,y)$ and $g_2(x,y)$ account for the effects of the transfer conductances in the reduced network. The existing energy functions for power systems with transfer conductances are not exact in the sense that they do not satisfy the three conditions of energy functions and they are not well defined functions. We term these functions *numerical energy functions*. We next propose a numerical energy function for the generic network-reduction model (13).

For the compact form of the network-reduction power system model (13), the numerical energy function $W(x,y,z)$ consists of two parts: an analytical energy function $W_{\text{ana}}(x,y,z) = \frac{1}{2}z^T M z + U(x,y)$ and a path-dependent potential energy $U_{\text{path}}(x,y)$, i.e.,

$$\begin{aligned} W(x,y,z) &= W_{\text{ana}}(x,y,z) + U_{\text{path}}(x,y) \\ &= K(z) + U(x,y) + U_{\text{path}}(x,y) \\ &= K(z) + U_{\text{num}}(x,y). \end{aligned}$$

For classical generator models, the path-dependent energy function can be expressed as

$$\begin{aligned} U_{\text{path}}(x,y) &= \sum_{i=1}^{n-1}\sum_{j=i+1}^{n} I_{ij} \\ &= \sum_{i=1}^{n-1}\sum_{j=i+1}^{n} \int V_i V_j G_{ij} \cos\delta_{ij}\, d(\delta_i + \delta_j). \end{aligned}$$

If a linear trajectory is assumed in the angle space, the above integration can be simplified as

$$I_{ij} = G_{ij}V_iV_j \frac{\delta_i + \delta_j - \delta_i^s - \delta_j^s}{\delta_i - \delta_j - \delta_i^s + \delta_j^s}[\sin\delta_{ij} - \sin\delta_{ij}^s]$$

Such an approximation is called the *ray approximation*. For a two-axis generator model with exciters, the numerical potential energy function can be written as the following equations [37], [72]:

$$U_{\text{num}}(x,y) = \int \sum_{i=1}^{n} \left[M_i\dot{\omega}_i - P_{mi} + P_{ei} - \frac{M_i}{M_T}P_{coi} \right] \dot{\delta}_i \, dt$$

where

$$\begin{aligned} P_{ei} &= E'_{di} i_{di} + E'_{qi} i_{qi}, \\ i_{di} &= \sum_{j=1}^{n} [F_{B-G}(\delta_{ij})E'_{qi} + F_{G+B}(\delta_{ij})E'_{di}], \\ i_{qi} &= \sum_{j=1}^{n} [F_{G+B}(\delta_{ij})E'_{qi} - F_{B-G}(\delta_{ij})E'_{di}], \\ F_{G+B}(\delta_{ij}) &= G_{ij}\cos\delta_{ij} + B_{ij}\sin\delta_{ij}, \quad \text{and} \\ F_{G-B}(\delta_{ij}) &= B_{ij}\cos\delta_{ij} - G_{ij}\sin\delta_{ij}. \end{aligned}$$

Numerical energy functions can be developed for other network-reduction models [58].

C. Computing the Controlling U.E.P.

The evolution of the concept of controlling u.e.p. (for the network-reduction model) can be traced back to the mid-1970's. In [61], Prabhakara and El-Abiad argued that the controlling u.e.p. is the u.e.p. which is closest to the fault-on trajectory. Athay *et al.* in [8] suggested that the controlling u.e.p. is the u.e.p. 'in the direction' of the fault-on trajectory. Ribbens–Pavella *et al.* [68] relate the controlling u.e.p. to the machine (or groups of machines) which first goes out of synchronism if the fault is sustained. Fouad *et al.* [35], associated the controlling u.e.p. with the 'mode of instability' of machines. These concepts have been used to develop several methods for computing the controlling u.e.p. The details of these methods can be found, for example in [37], [57], [58], [67]. These methods, however, have the following disadvantages: 1) the u.e.p.'s obtained by using these methods are not the exact controlling u.e.p. defined in the previous section, i.e. the first u.e.p. whose stable manifold is hit by the fault-on trajectory at the exit point. These methods have been found to give both overestimates and very conservative stability assessments in many cases, 2) they have no theoretical foundations, and 3) these methods do not have good convergence properties. Incidentally, several previous efforts in determining the critical energy value without computing the controlling u.e.p. can be found in [34], [44], [50], [84], [87].

Recently, a systematic method, called boundary of stability region based controlling unstable equilibrium point method (BCU method), to find the controlling u.e.p. was developed [15]–[17], [23]. The method was also given other names such as the exit point method [37], [62], [63] and the hybrid method [58]. The BCU method has been evaluated in a large-scale power system and it compared favorably with other methods in terms of its reliability and the required computational efforts [62], [63]. The BCU method has been applied to the fast derivation of power transfer limits [16] and to real power rescheduling to increase dynamic security [47], and demonstrated its capability for on-line transient stability assessments.

The fundamental ideas behind the BCU method can be explained in the following way. Given a power system stability model (which admits an energy function), the BCU method first explores special properties of the underlying model with the aim to define an artificial, dimension-reduction system such that the following conditions are met:

Static Properities:

- The locations of equilibrium points of the dimension-reduction system correspond to the locations of equilibrium points of the original system. For example, $(\hat{x},\hat{y})$ is an e.p. of the dimension-reduction system if and only if $(\hat{x},\hat{y},0)$ is an e.p. of the original system, where $0 \in R^m$, m is an appropriate positive integer.
- The types of equilibrium points of the dimension-reduction system are the same as those of the original system. For example, (x_s, y_s) is a stable equilibrium

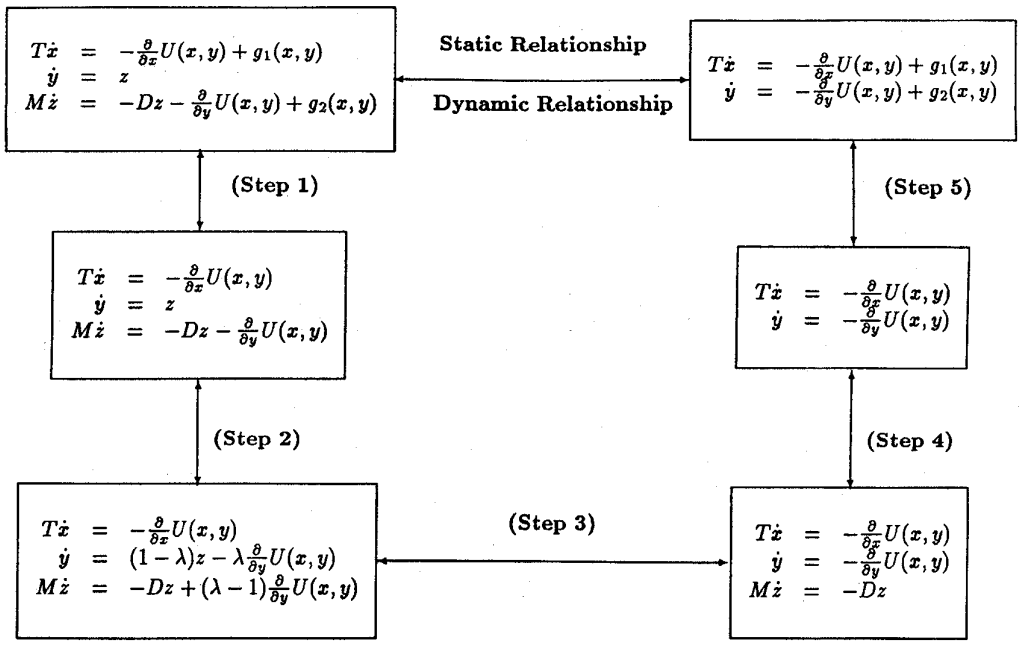

Fig. 21. A general procedure to determine the static and dynamic relationships between the network-reduction power system and the artificial, dimension-reduction system.

point of the dimension-reduction system if and only if $(x_s, y_s, 0)$ is a stable equilibrium point of the original system.

Dynamical Properties:

- There exists an energy function for the artificial, dimension-reduction system.
- An equilibrium point, say (x_i, y_i), is on the stability boundary $\partial A(x_s, y_s)$ of the dimension-reduction system if and only if the equilibrium point $(x_i, y_i, 0)$ is on the stability boundary $\partial A(x_s, y_s, 0)$ of the original system.
- It is much easier to identify the stability boundary $\partial A(x_s, y_s)$ of the dimension-reduction system than to identify the stability boundary $\partial A(x_s, y_s, 0)$ of the original system.

The BCU method then finds the controlling u.e.p. of the dimension-reduction system by exploring the special structure of the stability boundary and the energy function of the dimension-reduction system. Finally, it relates the controlling u.e.p. of the artificial system to the controlling u.e.p. of the original system.

D. Network-Reduction BCU Method

The main purpose of this subsection is to develop the BCU method for network-reduction power system models and to present a theoretical foundation for the developed methods.

Given a power system stability model, there exists a corresponding version of the BCU method. For the purpose of illustration, we consider the generic network-reduction power system model (13). To develop the BCU method for the generic model (13), we define the following system as the artificial, dimension-reduction system associated with the original system

$$\begin{aligned} T\dot{x} &= -\frac{\partial}{\partial x}U(x,y) + g_1(x,y) \\ \dot{y} &= -\frac{\partial}{\partial y}U(x,y) + g_2(x,y). \end{aligned} \tag{14}$$

A Conceptual Network Reduction Method:

Step 1: From the fault-on trajectory $(x(t), y(t), z(t))$, detect the exit point (x^*, y^*) at which the projected (fault-on) trajectory $(x(t), y(t))$ exits the stability boundary of the (postfault) dimension-reduction system (14).

Step 2: Use the point (x^*, y^*) as an initial condition and integrate the postfault dimension-reduction system (14) to find the controlling u.e.p. of the dimension-reduction system, say at (x^*_{co}, y^*_{co}).

Step 3: The controlling u.e.p. with respect to the fault-on trajectory $(x(t), y(t), z(t))$ is $(x^*_{co}, y^*_{co}, 0)$.

A nemerical implementation of the above conceptual network-reduction BCU method will be presented in Section VIII.

We next present a theoretical foundation for the above conceptual BCU method for the generic model (13). In doing so, we establish the static as well as dynamic relationships between the original system and the artificial dimension-reduction system via four intermediate systems summarized in Fig. 21. In each step identified in the figure, we determine the static as well as the dynamic relationship between the two systems. For instance, in Step 4 we determine the static and dynamic relationship between the

following system

$$T\dot{x} = -\frac{\partial}{\partial x}U(x,y)$$
$$\dot{y} = -\frac{\partial}{\partial y}U(x,y)$$

and the following system

$$T\dot{x} = -\frac{\partial}{\partial x}U(x,y)$$
$$\dot{y} = -\frac{\partial}{\partial y}U(x,y)$$
$$M\dot{z} = -Dz. \tag{15}$$

In Step 3 we determine the static as well as dynamic relationship between the following system

$$T\dot{x} = -\frac{\partial}{\partial x}U(x,y)$$
$$\dot{y} = -\frac{\partial}{\partial y}U(x,y)$$
$$M\dot{z} = -Dz$$

and the following one-parameter system $d(\lambda), 0 \leq \lambda \leq 1$

$$T\dot{x} = -\frac{\partial}{\partial x}U(x,y)$$
$$\dot{y} = (1-\lambda)z - \lambda\frac{\partial}{\partial y}U(x,y)$$
$$M\dot{z} = -Dz + (\lambda - 1)\frac{\partial}{\partial y}U(x,y). \tag{16}$$

Note that when $\lambda = 0$, the parametrized system $d(\lambda)$ is

$$T\dot{x} = -\frac{\partial}{\partial x}U(x,y)$$
$$\dot{y} = z$$
$$M\dot{z} = -Dz - \frac{\partial}{\partial y}U(x,y) \tag{17}$$

and when $\lambda = 1$, the system $d(\lambda)$ becomes

$$T\dot{x} = -\frac{\partial}{\partial x}U(x,y)$$
$$\dot{y} = -\frac{\partial}{\partial y}U(x,y)$$
$$M\dot{z} = -Dz. \tag{18}$$

Through the above procedure, we can derive the following analytic results regarding the relationship between the original system (13) and the dimension-reduction system (14).

Theorem 6-1 (Static relationship): Consider the original system (13) and the artificial dimension-reduction system (14). If zero is a regular value[7] of $(\partial^2 U/\partial x \partial y)(x,y)$, then there exists a positive number $\epsilon > 0$ such that if the transfer conductance of system (13) satisfies $G_{ij} < \epsilon$, $(\hat{x},\hat{y})$ is a type-k equilibrium point of the system (14) if, and only if $(\hat{x},\hat{y},0)$ is a type-k equilibrium point of the system (13).

[7]For a smooth map $f\colon X \to Y$, a point $y \in Y$ is called a regular value for f if $\partial f/\partial x$ is surjective at every point $x \in X$ such that $f(x) = y$.

Theorem 6-2 (Dynamic relationship): Let (x_s, y_s) be a stable equilibrium point of system (13). If zero is a regular value of $(\partial^2 U/\partial x \partial y)(x,y)$, then there exists a positive number $\epsilon > 0$ such that if the transfer conductance of system (13) satisfies $G_{ij} < \epsilon$ and the intersections of the stable and unstable manifolds of the equilibrium points on the stability boundary $\partial A(x_s, y_s)$ of the parameterized system $d(\lambda)$ satisfy the transversality condition for $\lambda \in [0,1]$, then

1) the equilibrium point $(x_i, y_i, 0)$ is on the stability boundary $\partial A(x_s, y_s, 0)$ of system (13) if, and only if the equilibrium point (x_i, y_i) is on the stability boundary $\partial A(x_s, y_s)$ of system (14); moreover,
2) the stability boundary $\partial A(x_s, y_s, 0)$ of system (12) is contained in the union of the stable manifold of the equilibrium points $(x_i, y_i, 0)$ on the stability boundary $\partial A(x_s, y_s, 0)$, i.e., $\partial A(x_s, y_s, 0) \subseteq \cup W^s(x_i, y_i, 0)$. The stability boundary $\partial A(x_s, y_s)$ of system (14) is contained in the union of the stable manifold of the equilibrium points (x_i, y_i) on the stability boundary $\partial A(x_s, y_s)$, i.e., $\partial A(x_s, y_s) \subseteq \cup W^s(x_i, y_i)$.

The analytical results derived in Theorem 6-2 support the plausibility of finding the controlling u.e.p. of the original system (13) via finding the controlling u.e.p. of the artificial, dimension-reduction system (14). We next present a sufficient condition under which the conceptual BCU method finds the correct controlling u.e.p. relative to a given fault: the exit point of the projected fault-on trajectory $(x(t), y(t))$ is on the stable manifold $W^s(\hat{x},\hat{y})$ if and only if $(x(t), y(t))$ is on the stable manifold $W^s(\hat{x},\hat{y},0)$. Theorem 6-2 shows that under the one-parameter transversality condition the equilibrium point $(\hat{x},\hat{y})$ is on the stability boundary $\partial A(\hat{x},\hat{y})$ of the dimension-reduction system (14) if and only if the equilibrium point $(\hat{x},\hat{y},0)$ is on the stability boundary $\partial A(\hat{x},\hat{y},0)$ of the original system (13). From a practical viewpoint, it would be useful to know whether or not the one-parameter transversality condition is always satisfied for practical power systems [49].

We next remark on the impact of using network-reduction power system models on the accuracy of transient stability analysis. First, load characteristics are known to have a significant effect on system dynamics. Inaccurate load modeling could lead to a power system operating in modes that result in actual system collapse or separation [27]. The so-called ZIP model (where the load is represented as a combination of constant impedance, constant current and constant MVA) are commonly used in current stability analysis programs. These static load models are adequate for some types of dynamic analysis but not for others (in which case, accurate complex static load models or dynamic load models are required). However, only the constant impedance load model (or equivalent model) is allowed in the network-reduction power system models. Hence, in the context of system modeling, the network-reduction power system models preclude consideration of load behaviors (i.e., voltage and frequency variations) at load buses. Second, in the context of physical explanation of results, re-

duction of the transmission network leads to loss of network topology and, hence, precludes study of transient energy shifts among different components of the entire power network. Network-preserving models (structure-preserving models) have been proposed in the last decade to overcome some of the shortcomings of the classical model and to improve the modeling of generators, exciters, automatic voltage regulators and load representations. We next discuss the direct methods for network-preserving power system models.

VII. Direct Methods for Network-Preserving Models

There are two advantages of using the network-preserving power system models for direct stability analysis. From a modeling viewpoint, it allows more realistic representations of power system components, especially load behaviors. From a computational viewpoint, it allows the use of the sparse matrix technique for the development of faster solution methods for solving nonlinear algebraic equations involved in direct methods [3], [4]. In this section we discuss direct methods for network-preserving power system models.

The first network-preserving model was developed by Bergen and Hill [10], who assumed frequency dependent real power demands and constant reactive power demands. Narasimhamurthi and Musavi [54] moved a step further by considering constant real power and voltage dependent reactive power loads. Padiyar and Sastry [56] have included nonlinear voltage dependent loads for both real and reactive powers. Tsolas, Araposthasis and Varaiya [75] developed a network-preserving model with the consideration of flux decay and constant real and reactive power loads. An energy function for a network-preserving model accounting for static var compensators and their operating limits was developed by Hiskens and Hill [43]. For purpose of illustration, we next discuss the Tsolas–Arapostathis–Varaiya model.

A. Model

In the Tsolas-Arapostathis-Varaiya model [75], [76], each generator is represented by the one-axis model. The transmission network representation is preserved. The complete dynamic equations are described in the following way.

1) *Internal Generator Bus:* one-axis generator model. For $i = 1, \cdots, n$,

$$\dot{\delta}_i = \omega_i$$

$$M_i\dot{\omega}_i = -D_i\omega_i + P_{mi} - P_{ei}$$

$$T'_{do}\dot{E}'_{qi} = -\frac{x_{di}}{x'_{di}}E'_{qi} + \frac{x_{di} - x'_{di}}{x'_{di}}V_i\cos(\delta_i - \theta_i) + E_{fi}$$

where

$$P_{ei} = \frac{1}{x'_{di}}E'_{qi}V_i\sin(\delta_i - \theta_i) + \frac{x'_{di} - x_{qi}}{2x_{qi}x'_{di}}V_i^2\sin[2(\delta_i - \theta_i)].$$

2) *External Generator Bus:* For $i = 1, \cdots, n$,

$$\begin{aligned} P_{ei} = &\sum_{j\neq i}^{n+1} V_iV_j(B_{ij}\sin(\theta_i - \theta_j) \\ &+ G_{ij}\cos(\theta_i - \theta_j)) \\ &+ \sum_{l=n+2}^{n+m+1} V_iV_l(B_{il}\sin(\theta_i - \theta_l) \\ &+ G_{il}\cos(\theta_i - \theta_l)) \\ 0 = &\frac{x'_{di} + x_{qi}}{2x_{qi}x'_{di}}V_i^2 - \frac{E'_{qi}V_i}{x'_{di}}\cos(\theta_i - \delta_i) \\ &- \frac{x'_{di} - x_{qi}}{2x_{qi}x'_{di}}V_i^2\cos[2(\theta_i - \delta_i)] \\ &- \sum_{j=1}^{n+1} V_iV_j(B_{ij}\cos(\theta_i - \theta_j) \\ &+ G_{ij}\sin(\theta_i - \theta_j)) \\ &- \sum_{l=n+2}^{n+m+1} V_iV_l(B_{il}\cos(\theta_i - \theta_l) \\ &+ G_{il}\sin(\theta_i - \theta_l)). \end{aligned}$$

3) *Load Bus:* For $k = n+2, \cdots, n+m+1$,

$$\begin{aligned} P_k^d - D_k\dot{\theta}_k = &\sum_{j=1}^{n+m+1} V_kV_j(B_{kj}\sin(\theta_k - \theta_j) \\ &+ G_{kj}\cos(\theta_k - \theta_j)) \\ Q_k^d(V_k) = &-\sum_{j=1}^{n+m+1} V_kV_j(B_{kj}\cos(\theta_k - \theta_j) \\ &+ G_{kj}\sin(\theta_k - \theta_j)). \end{aligned}$$

The above model is a network-preserving power system transient stability model. In general, network-preserving models are mathematically described by a set of differential and algebraic equations (DAE's):

$$\begin{aligned} \dot{x} &= f(x, y) \\ 0 &= g(x, y) \end{aligned} \tag{19}$$

where $x \in R^n$ and $y \in R^m$. Here differential equations describe generator and/or load dynamics while algebraic equations express the power flow equations at each bus. The above DAE system can be interpreted as an implicitly dynamical system on the algebraic manifold L

$$L = \{(x, y)\colon g(x, y) = 0\}.$$

It has been shown that a DAE in general can be reduced locally to an ODE [12]. However, despite the strong analogy between DAE's and ODE's, major differences do exist. For instance, once the trajectory intersects the following *singular surface* S,

$$S = \left\{(x, y)\colon (x, y) \in L, \Delta(x, y) = \det\frac{\partial}{\partial y}g(x, y) = 0\right\}$$

a DAE can not be reduced to an ODE. From a dynamical viewpoint, complicated dynamic behaviors will occur in

the vicinity of S. For instance, most of the trajectories near singular surfaces will not exist beyond singular surfaces; only when the initial conditions of the DAE satisfy certain conditions, the trajectories can be extended further [25]. Due to their intricate complicated dynamics near singular surfaces, DAE systems are difficult to analyze and only some phenomena are completely understood. We next discuss some analytical results for DAE systems that are useful for stability analysis of network-preserving power system models.

B. DAE Systems

If the Jacobian $(\partial/\partial y)g(x,y)$ is nonsingular, i.e, the system is on the *regular* part of the DAE (19), then by the Implicit Function Theorem [2, p. 40], the system equations (19) are locally equivalent to the following equations:

$$\begin{aligned}\dot{x} &= f(x,y)\\ \dot{y} &= -\left(\frac{\partial}{\partial y}g(x,y)\right)^{-1}\frac{\partial}{\partial x}g(x,y)f(x,y).\end{aligned} \tag{20}$$

The existence and uniqueness of solutions of DAE in a neighborhood N of the initial conditions can be guaranteed provided functions f and g are smooth and the Jacobian $(\partial/\partial y)g(x,y)$ has a full rank on N [41]. An equilibrium point of system (19) is a point such that $f(x,y)=0$ and $g(x,y)=0$. A regular equilibrium point is called a *type-k* equilibrium point if the corresponding equilibrium point of system (20) is a type-k equilibrium point. The stability of an equilibrium point of the DAE (19) can be analyzed by using a local energy function. The following lemma summarizes this result.

Lemma 7-1: [41] (Stability of an Equilibrium Point). Let $(\overline{x},\overline{y})$ be an equilibrium point of system (19) and N be a small neighborhood of $(\overline{x},\overline{y})$ in the algebraic manifold $\{(x,y)\colon g(x,y)=0\}$. If there exists a smooth positive definite function $V\colon N\to R$ such that

$$\begin{aligned}\dot{V} = &\frac{\partial}{\partial x}V(x,y)f(x,y) - \frac{\partial}{\partial y}V(x,y)\\ &\cdot\left(\frac{\partial}{\partial y}g(x,y)\right)^{-1}\frac{\partial}{\partial x}g(x,y)f(x,y) \le 0\end{aligned}$$

then the equilibrium point $(\overline{x},\overline{y})$ is stable.

Hill and Mareels applied the above result to analyze network-preserving power systems [41]. Later, Hiskens and Hill utilized the same framework to establish a connection between transient stability, multiple stable equilibria and voltage behaviors [43]. However, it is usually very difficult to generalize these local results into global results because once the trajectory intersects the singular surface S, the implicit function theorem does not apply and some elements of the vector field become unbounded.

The singular surface S decomposes the algebraic manifold L into several disjoint components Γ_i. If all the points on some Γ_i so that the Jacobian matrix $(\partial/\partial x)g(x,y)$ has eigenvalues with negative real parts, then Γ_i is called a *stable* component; otherwise, it is called an *unstable* component. Since the vector field is unbounded on the singular surface, it can be expected that trajectories move very fast near the singular surface. Once the trajectory reaches the singular surface, an un-smooth jump behavior will occur and force the trajectory to reach another adjacent piece of the algebraic manifold. A comprehensive analysis of the dynamic behaviors near the singular surface can be found in [77]–[79].

We next discuss the concept of the stability region for DAE systems. Let Γ_s be a stable component of L and $\Phi(t)$ be a trajectory of the DAE system (19), then the *stability region* of a given stable equilibrium point (x_s,y_s) of a DAE system (19) is defined as

$$A(x_s,y_s) = \{(x,y)\in\Gamma_s\colon \lim_{t\to\infty}\Phi(t) = (x_s,y_s)\}.$$

Here we restrict the stability region to lie on the stable component Γ_s and exclude the possibility that there may exist a trajectory which starts from an initial condition lying on another stable component, passes through the singular surface and converges to the stable equilibrium point (x_s,y_s). Similarly, the stable manifold and the unstable manifold of an equilibrium point $(\overline{x},\overline{y})$ on Γ_s are defined as follows:

$$\begin{aligned}W^s(\overline{x},\overline{y}) &= \{(x,y)\in\Gamma_s\colon \lim_{t\to\infty}\Phi(t) = (\overline{x},\overline{y})\}\\ W^u(\overline{x},\overline{y}) &= \{(x,y)\in\Gamma_s\colon \lim_{t\to-\infty}\Phi(t) = (\overline{x},\overline{y})\}.\end{aligned}$$

Characterizations of the stability boundary $\partial A(x_s,y_s)$ of a stable equilibrium point (x_s,y_s) of a DAE system have been studied recently. Chiang *et al.* show that under certain moderate conditions, the stability boundary $\partial A(x_s,y_s)$ consists of two parts: the first part is the stable manifolds of the equilibrium points on the stability boundary while the second part contains points whose trajectories reach singular surfaces [26]. Venkatasubramanian *et al.* further delineated the second part with various dynamic behaviors near the singular surface and show the stability boundary can be characterized as a union of the stable manifolds of unstable equilibrium points, pseudo-equilibrium points and semi-singular points on the stability boundary and parts of singular surface [77].

As pointed out earlier, methods based on energy functions are more suitable for estimating stability regions of large-scale nonlinear systems. Regarding the applicability of the energy function theory to DAE systems, it is usually very difficult to generalize a local energy function into a global energy function for DAE systems. We propose to use the singular perturbation approach to bridge the gap between the DAE system and the energy function theory.

C. Singular Perturbation Systems

The singular perturbation approach is widely investigated in applied mathematics and control system societies [45], [55]. The application of such concepts in network-preserving power system models was initiated by Sastry *et al.* [70], [71], and considered later by Arapostathis *et al.* [7], Bergen *et al.* [10], [11], De Marco *et al.* [28], [29] and Chiang *et al.* [18]. This approach treats algebraic equations

as a limit of the fast dynamics: $\epsilon\dot{y} = g(x, y)$. In other words, as ϵ approaches zero, the fast dynamics will approach the algebraic manifold. Therefore, for the DAE system (19), we can define an associated singularly perturbed system

$$\begin{aligned} \dot{x} &= f(x, y) \\ \epsilon\dot{y} &= g(x, y) \end{aligned} \tag{21}$$

where ϵ is a sufficiently small positive number. If f and g are both smooth functions and bounded for all $(x, y) \in R^{n+m}$, then the vector field is globally well defined. The very different rates shown in the system can be separated in two distinct time scales: slow variable x and fast variable y. The effects of the sign in the algebraic equations for power system applications are worth recognizing: the algebraic manifold remains invariant whether there is a positive sign or a negative sign in front of $g(x, y)$. However, this sign will affect significantly the dynamical behaviors of corresponding singularly perturbed system. It is therefore imperative to choose a proper sign in algebraic equations to represent an appropriately corresponding singularly perturbed system.

Although the DAE system and the corresponding singularly perturbed system have some different dynamic models, they still share several similar dynamical properties. The following results demonstrate the invariant topological structure among equilibrium points between a DAE system and the associated singularly perturbed system.

Fact:

The equilibrium points of the DAE system (19) are the same as the equilibrium points of the singularly perturbed system (21).

Lemma 7-3: Suppose that all of the equilibrium points of interest are on one stable component Γ_s. Then there exists an $\epsilon^* > 0$ such that for all $\epsilon \in (0, \epsilon^*)$,

1) $(\overline{x}, \overline{y})$ is a hyperbolic equilibrium point of the DAE system (19) if and only if $(\overline{x}, \overline{y})$ is a hyperbolic equilibrium point of the singularly perturbed system (21).
2) For $k \leq n$, $(\overline{x}, \overline{y})$ is a *type-k* equilibrium point of the DAE system (19) if and only if $(\overline{x}, \overline{y})$ is a *type-k* equilibrium point of the singularly perturbed system (21).

The above lemma shows that the type of the equilibrium point of the DAE system (19) is the same as the type of the corresponding equilibrium point of the singularly perturbed system (21) provided ϵ is sufficiently small. Theorem 7-4 below generalizes this result and shows that the stability boundaries of such two systems contain the same set of equilibrium points on the stable component Γ_s.

Theorem 7-4 [18], [33]: Let (x_s, y_s) and (x_u, y_u) be the stable and unstable equilibrium points of the DAE system (19) on the stable component Γ_s, respectively. Suppose that for each $\epsilon > 0$, the associated singularly perturbed system (21) has an energy function and every equilibrium point is isolated. Then there exists $\epsilon^* > 0$ such that for all $\epsilon \in (0, \epsilon^*)$, (x_u, y_u) lies on the stability boundary of the DAE system $\partial A_0(x_s, y_s)$ if and only if (x_u, y_u) lies on the stability boundary of the singularly perturbed system $\partial A_\epsilon(x_s, y_s)$.

Stability analysis of network-preserving models via the singular perturbation approach does provide some advantages in the following aspects:

1) *Energy function:* The energy function of the network-preserving model can be easily obtained and the global analysis of the vector field can be extended.
2) *Computing the controlling u.e.p.:* Since the final state of the fault-on system will not lie on the algebraic manifold L of the postfault system, the fault-on trajectory will not hit the stability boundary of its DAE postfault system. Instead, the fault-on trajectory will hit the stability boundary of its corresponding singularly perturbed postfault system. Hence the exit point of a fault-on trajectory must lie on the stable manifold of the controlling u.e.p. of the singularly perturbed postfault system.
3) *Solution trajectory:* Trajectories of the singularly perturbed system (21) will not be confined to the algebraic manifold L and they are not exactly the same as trajectories of the original DAE system. However, the Tikhonov's theorem over the infinite time interval can be applied to provide a theoretical justification to ensure that the difference of solution trajectories between the original DAE system (19) and the singularly perturbed system (21) is uniformly bounded by the order of $O(\epsilon)$ [45]. Thus trajectories generated by the singular perturbed system are still valid approximations to that of the DAE system.

D. Exact and Numerical Energy Functions

All existing network-preserving models can be written as a set of general differential-algebraic equations of the following compact form:

$$\begin{aligned} 0 &= -\frac{\partial}{\partial u}U(u, w, x, y) + g_1(u, w, x, y) \\ 0 &= -\frac{\partial}{\partial w}U(u, w, x, y) + g_2(u, w, x, y) \\ T\dot{x} &= -\frac{\partial}{\partial x}U(u, w, x, y) + g_3(u, w, x, y) \\ \dot{y} &= z \\ M\dot{z} &= -Dz - \frac{\partial}{\partial y}U(u, w, x, y) + g_4(u, w, x, y) \end{aligned} \tag{22}$$

where $u \in T^k$ and $w \in R^l$ are instantaneously variables while $x \in R^n$, $y \in T^n$, and $z \in R^n$ are state variables. T is a positive definitive matrix and M and D are diagonal positive definite matrices. $g_1(u, w, x, y)$, $g_2(u, w, x, y)$, $g_3(u, w, x, y)$, and $g_4(u, w, x, y)$ are the vector field representing the effects of the transfer conductance in the network Y-bus matrix.

To avoid an awkward analysis of the DAE representation, the algebraic equations can be treated as the limiting equations of the singularly perturbed differential equations. The compact representation of the network-preserving model

Table 2 Coordinates of Type-One and Type-Two Equilibrium Points

Type-One e.p.	δ_1	ω_1	δ_2	ω_2	Type-Two e.p.	δ_1	ω_1	δ_2	ω_2
1	3.24512	0	0.31170	0	1	3.60829	0	1.58620	0
2	3.04037	0	3.24307	0	2	2.61926	0	4.25636	0
3	0.03333	0	3.10823	0	3	−2.67489	0	1.58620	0
4	−3.03807	0	0.3117	0	4	−3.66392	0	−2.02684	0
5	-3.24282	0	−3.03931	0	5	−2.67489	0	−4.69699	0
6	0.03333	0	−3.17496	0	6	2.61926	0	−2.02684	0

thus becomes:

$$\begin{aligned}
\epsilon_1\dot{u} &= -\frac{\partial}{\partial u}U(u,w,x,y) + g_1(u,w,x,y)\\
\epsilon_2\dot{w} &= -\frac{\partial}{\partial w}U(u,w,x,y) + g_2(u,w,x,y)\\
T\dot{x} &= -\frac{\partial}{\partial x}U(u,w,x,y) + g_3(u,w,x,y)\\
\dot{y} &= z\\
M\dot{z} &= -Dz - \frac{\partial}{\partial y}U(u,w,x,y) + g_4(u,w,x,y) \quad (23)
\end{aligned}$$

where ϵ_1 and ϵ_2 are sufficiently small positive numbers.

If $g_1(u,w,x,y)$, $g_2(u,w,x,y)$, $g_3(u,w,x,y)$, and $g_4(u,w,x,y)$ are zero, the compact representation of the network-preserving model will become:

$$\begin{aligned}
\epsilon_1\dot{u} &= -\frac{\partial}{\partial u}U(u,w,x,y)\\
\epsilon_2\dot{w} &= -\frac{\partial}{\partial w}U(u,w,x,y)\\
T\dot{x} &= -\frac{\partial}{\partial x}U(u,w,x,y)\\
\dot{y} &= z\\
M\dot{z} &= -Dz - \frac{\partial}{\partial y}U(u,w,x,y). \quad (24)
\end{aligned}$$

If we define

$$W(u,w,x,y,z) = \tfrac{1}{2}z^T Mz + U(u,w,x,y)$$

then $W(u,w,x,y,z)$ is an energy function. Indeed, by differentiating $W(u,w,x,y,z)$ along the trajectory, one has

$$\begin{aligned}
\dot{W}(u,w,x,y,z) &= \frac{\partial W^T}{\partial u}\dot{u} + \frac{\partial W^T}{\partial w}\dot{w} + \frac{\partial W^T}{\partial x}\dot{x}\\
&\quad + \frac{\partial W^T}{\partial y}\dot{y} + \frac{\partial W^T}{\partial z}\dot{z}\\
&= -\epsilon_1^{-1}\frac{\partial U^T}{\partial u}\frac{\partial U}{\partial u} - \epsilon_2^{-1}\frac{\partial U^T}{\partial w}\partial U\partial w\\
&\quad - \frac{\partial U^T}{\partial x}T^{-1}\frac{\partial U}{\partial x} - z^T Dz \le 0. \quad (25)
\end{aligned}$$

Therefore, the condition (1) of the energy function is satisfied. Suppose that there is an interval $t \in [t_1, t_2]$ such that $\dot{W}(u(t), w(t), x(t), y(t), z(t)) = 0$. It follows from (24) and (25) that $z(t) = 0$ and $\dot{u}(t) = \dot{w}(t) = \dot{x}(t) = 0$ for $t \in [t_1, t_2]$. This indicates that $y(t)$ is a constant for $t \in [t_1, t_2]$. It then follows that the system state is at an equilibrium point. Thus condition (2) of the energy function also holds. We can employ similar arguments used for the network-reduction model to show that condition (3) is also true; here we omit the detailed proof. Note that the additional terms in $\dot{W}(u,w,x,y,z)$, as compared with those in the network-reduction model, are related to the energy dissipation at load buses. Moreover, as ϵ approaches zero, these terms become dominant in $\dot{W}(u,w,x,y,z)$. This observation also shows the important role of load models for stability analysis. When the network transfer conductance is not negligible, a general expression of exact energy functions does not exist. In this case, path-dependent numerical energy functions may prove adequate. This is similar to the case for network-reduction models. However, the transfer conductances of the network-preserving models are usually much smaller in relative value than that of the network-reduction models. This physical property makes numerical energy functions for network-preserving models 'close' to exact energy functions. This illustrates another advantage of using network-preserving models instead of using network-reduction models.

E. Controlling U.E.P. Method

The controlling u.e.p. of the generic network-preserving model (22) can be found via the controlling u.e.p. of the associated singularly perturbed system (23). In order to make this picture more precise, the relationship between the postfault trajectory of the associated singularly perturbed model and that of the postfault network-preserving model needs to be established. With the aid of the singularly perturbed system, it can be shown that the postfault trajectory of the DAE system is approximately equal to the trajectory generated by the singularly perturbed system under mild conditions. This suggests that one can detect the controlling u.e.p. of the singularly perturbed system and use the constant energy surface passing the controlling u.e.p. of the singularly perturbed system as the relative stability boundary for the fault-on trajectory of network-preserving models. Once the fault-on trajectory is inside the energy surface, the trajectory generated by the DAE system will converge to the stable equilibrium point of the postfault DAE system. Thus the controlling u.e.p. of the singularly perturbed system can be used for stability analysis of the network-preserving model.

We next present the controlling u.e.p. method for transient stability analysis of network-preserving models:

1) Determination of the critical energy
   Step 1.1: Find the controlling u.e.p. $(u_{co}, w_{co}, x_{co}, y_{co}, 0)$ relative to the fault-on DAE trajectory via its associated singularly perturbed system.

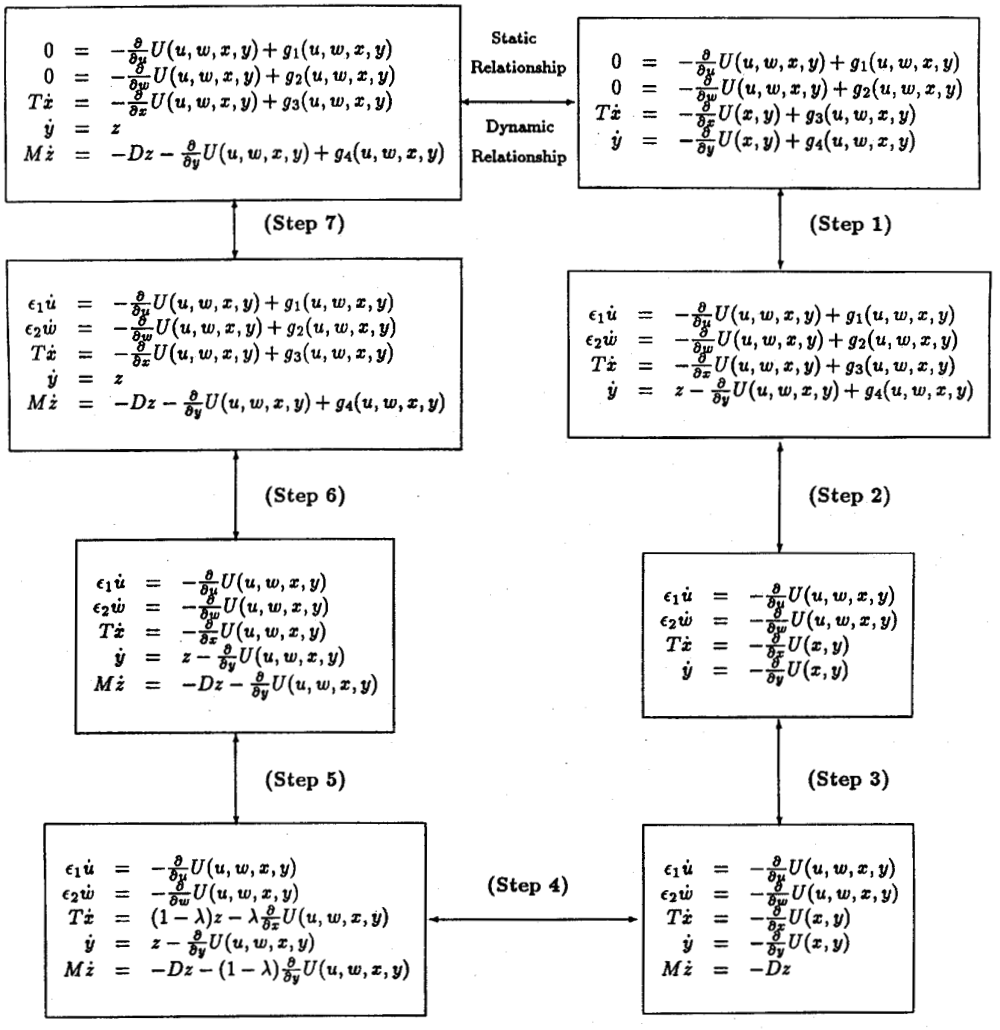

Fig. 22. A general procedure to determine the static and dynamic relationships between the generic network-preserving power system and the artificial, dimension-reduction system.

Step 1.2: The critical energy value W_{cr} is the value of energy function $W(\cdot,\cdot,\cdot,\cdot,\cdot)$ at the controlling u.e.p., i.e., $W_{cr} = W(u_{co}, w_{co}, x_{co}, y_{co}, 0)$.

2) Determination of stability

Step 2.1: Calculate the value of the energy function $W(\cdot,\cdot,\cdot,\cdot,\cdot)$ at the time of fault clearance (say t_{cl}) using the fault-on DAE trajectory $W_f = W((u_f(t_{cl}), w_f(t_{cl}), x_f(t_{cl}), y_f(t_{cl}), z_f(t_{cl}))$.

Step 2.2: If $W_f < W_{cr}$, then the postfault system is stable. Otherwise, it may be unstable.

The key step in the above controlling u.e.p. method is Step 1.1. In the next subsection, a network-preserving BCU method which finds the controlling u.e.p. of the corresponding singularly perturbed system will be presented.

F. A Network-Preserving BCU Method

To develop a BCU method for the generic network-preserving model (22), the associated artificial dimension-reduction system needs to be defined first. We choose the following differential-algebraic system as our dimension-reduction system:

$$\begin{aligned} 0 &= -\frac{\partial}{\partial u}U(u,w,x,y) + g_1(u,w,x,y) \\ 0 &= -\frac{\partial}{\partial w}U(u,w,x,y) + g_2(u,w,x,y) \\ T\dot{x} &= -\frac{\partial}{\partial x}U(u,w,x,y) + g_3(u,w,x,y) \\ \dot{y} &= -\frac{\partial}{\partial y}U(u,w,x,y) + g_4(u,w,x,y). \end{aligned} \tag{26}$$

We propose to establish the static as well as dynamic relationship between the dimension-reduction DAE system (26) and the the original DAE system via seven steps and six intermediate systems shown in Fig. 22. By combining the relationship between Steps 1–7, the following analytic results can be established.

Theorem 7-5 (Static relationship): Let (u_s, w_s, x_s, y_s) be a stable equilibrium point of system (26). If zero is a regular value of $\partial^4 U(u,w,x,y)/\partial u \partial w \partial x \partial y$, then there exists a

Table 3 Simulation Results of the 50-Generator, 145-Bus IEEE Test System Modeled by the Network Reduction, Classical Generators Power System Model. The Case Marked * is More Stressed Than the Other Cases Which Leads to Multiswing Trajectories. The Sign ** Means that the Corresponding Method Does Not Converge to a u.e.p. in that Case

Faulted Bus	Opened Line	ETMSP Method	BCU Method	Error (%)	MOD Method	Error (%)	Exit Point Method	Error (%)	Hybrid Method	Error (%)	Mixed DEEAC Method	Error (%)
7	7-6	108.2	102.0	-5.73	112.5	3.9	112.5	3.9	107.5	-0.7	108	-0.18
7*	7-6	107.5	106.2	-1.2	127.5	18.6	142.5	32.6	107.5	0.0	118	9.7
59	59-72	224.5	224.1	-0.18	242.5	8.0	197.5	-12.0	222.5	-0.9	227	1.3
73	73-84	215.5	194.2	-9.88	**	**	**	**	207.5	-3.7	209	-3.0
112	112-69	248.6	235.4	-5.63	237.5	-4.4	237.5	-4.4	247.5	-0.4	246	-1.0
66	66-67	171.0	160.2	-6.31	**	**	**	**	162.5	-5.0	165	-3.5
115	115-116	292.5	288.3	-1.43	287.5	-1.7	287.5	-1.7	292.5	0.0	291	-0.5
100	100-72	260.0	253.6	-2.46	252.9	-2.9	252.9	-2.9	257.5	-1.0	261	0.4
101	101-73	248.0	238.2	-3.95	237.5	-3.5	237.5	-3.5	247.5	0.6	244	-0.8
91	91-75	188.0	187.7	-0.15	187.5	-0.3	187.5	-0.3	187.5	-0.3	190	1.06
6	6-1	171.0	155.0	-9.3	**	**	237.5	38.9	167.5	-2.0	162	-5.2
12	12-14	173.5	163.0	-6.1	**	**	**	**	172.5	-0.6	168	-3.1
6	6-10	177.0	165.0	-6.8	**	**	**	**	172.5	-2.5	173	-2.2
33	33-39	386.0	385.0	-0.3	**	**	347.5	-10.0	382.5	-0.9	383	-0.8
33	33-49	387.5	387.0	-0.1	432.5	11.6	347.5	-10.3	382.5	-1.3	383	-0.8
66	66-111	175.5	163.5	-6.8	**	**	**	**	167.5	-4.6	168	-4.2
106	106-74	185.5	172.0	-7.3	-172.5	-7.0	172.5	-7.0	182.5	-1.6	181	-2.4
69	69-32	205.3	186.2	-9.3	**	**	**	**	202.5	-1.4	203	-1.1
69	69-112	205.1	185.0	-9.8	**	**	**	**	207.5	1.2	199	-2.9
105	105-73	213.5	206.5	-3.3	**	**	**	**	207.5	-2.8	207	-3.0
73	73-75	215.1	196.0	-8.9	**	**	**	**	212.5	-1.2	209	-2.8
67	67-65	233.7	227.4	-2.7	**	**	**	**	232.5	-0.5	199	-14.8
59	59-103	222.6	220.0	-1.7	**	**	242.5	8.9	222.5	-0.0	227	2.0
12	12-14, 12-14	169.7	160.0	-5.7	**	**	**	**	167.5	-1.3	165	-2.8
105	105-73, 105-73	120.0	114.0	-5.0	127.5	6.3	127.5	6.3	117.5	-2.0	127	5.8

positive number $\epsilon > 0$ such that the transfer conductance of system (26) satisfies $G_{ij} < \epsilon$, hence $(\hat{u}, \hat{w}, \hat{x}, \hat{y})$ is a type-k equilibrium point of system (26) if and only if $(\hat{u}, \hat{w}, \hat{x}, \hat{y}, 0)$ is a type-k equilibrium point of the system (22).

Theorem 7-6 (Dynamic relationship): Let (u_s, w_s, x_s, y_s) be a stable equilibrium point of system (26) and zero be a regular value of $\partial^4 U(u, w, x, y)/\partial u \partial w \partial x \partial y$. If there exists a positive number $\epsilon > 0$ such that the transfer conductance of system (26) satisfies $G_{ij} < \epsilon$ and the intersections of the stable and unstable manifolds of the equilibrium points on the stability boundary $\partial A(u_s, w_s, x_s, y_s, 0)$ of the parameterized system $d(\lambda)$ satisfy the transversality condition for $\lambda \in [0, 1]$, then

1) the equilibrium point $(u_i, w_i, x_i, y_i, 0)$ is on the stability boundary $\partial A(u_s, w_s, x_s, y_s, 0)$ of system (26) if and only if the equilibrium point $(u_i, w_i, x_i, y_i, 0)$ is on the stability boundary $\partial A(u_s, w_s, x_s, y_s, 0)$ of system (22).
2) The stability boundary $\partial A(u_s, w_s, x_s, y_s, 0)$ of system (22) is the union of the stable manifold of the equilibrium points $(u_i, w_i, x_i, y_i, 0)$ on the stability boundary $\partial A(u_s, w_s, x_s, y_s, 0)$, i.e.,

$$\partial A(u_s, w_s, x_s, y_s, 0) = \bigcup W^s(u_i, w_i, x_i, y_i, 0).$$

The stability boundary $\partial A(u_s, w_s, x_s, y_s)$ of system (26) is contained in the union of the stable manifold of the equilibrium points (u_i, w_i, x_i, y_i) on the stability boundary $\partial A(u_s, w_s, x_s, y_s)$, i.e.,

$$\partial A(u_s, w_s, x_s, y_s) = \bigcup W^s(u_i, w_i, x_i, y_i).$$

Theorems 7-5 and 7-6 provide a theoretical basis for finding the controlling u.e.p. of the original network-preserving model via the controlling u.e.p. of the artificial, dimension-reduction model. Based on the above theoretical developments, a conceptual BCU method for the network-preserving model is presented in the following:

G. A Conceptual Network-Preserving BCU Method

Step 1: From the fault-on trajectory $(u(t), w(t), x(t), y(t), z(t))$ of the original system, detect the exit point (u^*, w^*, x^*, y^*) at which the projected (fault-on) trajectory $(u(t), w(t), x(t), y(t))$ of the original system exits the stability boundary of the postfault dimension-reduction system.

Step 2: Use the point (u^*, w^*, x^*, y^*) as the initial condition and integrate the postfault dimension-reduction system (26) to find the controlling u.e.p. of the postfault dimension-reduction system, say $(u^*_{co}, w^*_{co}, x^*_{co}, y^*_{co})$.

Step 3: The controlling u.e.p. with respect to the fault-on trajectory $(u(t), w(t), x(t), y(t))$ of the original system is $(u^*_{co}, w^*_{co}, x^*_{co}, y^*_{co}, 0)$.

Recall that the essence of the BCU method is that it finds the controlling u.e.p. of the original system via the controlling u.e.p. of the dimension-reduction system whose controlling u.e.p. is easier to compute. Step 1 and Step 2

Table 3 *(Continued)*

Faulted Bus	Opened line	ETMSP Method	BCU Method	Error (%)	MOD Method	Error (%)	Exit Point Method	Error (%)	Hybrid Method	Error (%)	Mixed DEEAC Method	Error (%)
66	66-8, 66-8	178.5	171.0	−4.2	**	**	**	**	167.5	−6.2	173	−3.1
6	6-1, 6-2, 6-7	39.4	39.2	−0.5	72.5	84.0	52.5	33.2	22.5	−42.9	—	—
6	6-9, 6-10, 6-12, 6-12	81.5	77.0	−5.5	**	**	>500	**	77.5	−4.9	69	−15.3
33	33-37, 33-38, 33-39, 33-40, 33-49, 33-50	360.5	355.0	−1.4	>600	**	>700	**	352.5	−2.2	344	−4.5
33	33-37, 33-38, 33-39, 33-40	378	373.4	−1.2	352.5	−6.7	>700	**	372.5	−1.5	368	−2.6
66	66-111, 66-111, 66-111	83.0	80.0	−3.6	**	**	112.5	35.5	82.5	−0.6	82	−1.2
73	73-26, 73-72, 73-82, 73-101	214.5	195.0	−9.1	**	**	**	**	207.5	−3.3	209	−2.5
73	73-69, 73-75, 73-91, 73-96, 73-109	190.5	190.1	−0.20	**	**	77.5	−59.3	187.5	−1.6	179	−6.0

of the conceptual BCU method find the controlling u.e.p. of the dimension-reduction system and Step 3 relates the controlling u.e.p. of the dimension-reduction system to the controlling u.e.p. of the original system.

VIII. Numerical Aspects of BCU Methods

This section presents practical numerical implementations of BCU methods for both network-reduction models and network-preserving models. The numerical BCU methods are then applied to two sets of practical power system data. Practical demonstrations of the BCU method for on-line transient stability assessment will be described in the next section.

A. A Numerical Network-Reduction BCU Method

A numerical implementation of the conceptual BCU method for network-reduction power system models discussed in Section VI—D is proposed below.

Step 1: From the (sustained) fault-on trajectory $(x(t), y(t), z(t))$,[8] compute the exit point (x^*, y^*) at which the projected trajectory $(x(t), y(t))$ reaches its first local maximum of the numerical potential energy $U_{\text{num}}(\cdot, \cdot)$.

Step 2: Use the point (x^*, y^*) as the initial condition and integrate the postfault dimension-reduction system (14) to the (first) local minimum of $\|-(\partial/\partial x)U(x,y)+g_1(x,y)\|+\|-(\partial/\partial y)U(x,y)+g_2(x,y)\|$. Let the local minimum be (x_o^*, y_o^*).

[8]When the fault is cleared, the projected fault-on trajectory may not exit the stability boundary of the postfault dimension-reduction system. However, it must exit the stability boundary if the fault is sustained.

Step 3: Use the point (x_o^*, y_o^*) as the initial guess and solve the following set of nonlinear algebraic equations

$$\| -\frac{\partial}{\partial x}U(x,y) + g_1(x,y)\| + \| -\frac{\partial}{\partial y}U(x,y) + g_2(x,y)\|$$

Let the solution be (x_{co}^*, y_{co}^*).

Step 4: The controlling u.e.p. with respect to the fault-on trajectory $(x(t), y(t), z(t))$ is $(x_{co}^*, y_{co}^*, 0)$.

Remarks: There are basically three major computational tasks in the BCU method: 1) compute the point with the first local maximum of potential energy along the projected fault-on trajectory, 2) compute the trajectory of the postfault dimension-reduction system until the first local minimum is reached, and 3) compute the controlling u.e.p. via solving the nonlinear algebraic equations of the postfault dimension-reduction system.

The heuristic criterion that along the projected trajectory $(x(t), y(t))$, the first local maximum of the numerical potential energy $U_{\text{num}}(\cdot, \cdot)$ occurs at the exit point of the projected fault-on trajectory is used in Step 1 to compute the exit point. We have found through our numerical experience that the heuristic criterion works quite well.

The dimension-reduction system (14) can be stiff. In such a case, a stiff differential equation solver is recommended to implement Step 2.

There is no quarantee that the point with the (first) local minimum is always suuficiently close to the controlling u.e.p.; especially when the stability boundary of the postfault dimension-reduction system is very "ragged." In this case, techniques can be developed to circumvent this difficulty.

Table 4 Simulation Results of the 50-Generator, 145-Bus IEEE Test System Modeled by the Network-Reduction, Two-Axis Generator with a First-Order Exciter Power System Model

Faulted Bus	Opened Line	CCT BCU	CCT ETMSP	Relative Error (%)
59	59-72	210	224	−6.25
112	112-69	230	248	−7.3
115	115-116	287	288	−1
101	101-73	233	246	−5.25
106	106-74	123	174	−29
102	63-102	184	202	−9.00
97	97-66	244	261	−6.51
98	98-72	186	206	−9.70
108	108-75	264	279	−3.65
82	82-75	265	314	−15.6
100	100-72	245	259	−4.30
103	103-59	255	300	−15.0
89	89-59	250	274	−9.70
135	135-138	130	136	−4.50

It is likely that other versions of numerical implementation of the conceptual BCU method will appear in the future. Numerical experience with the above numerical BCU method on some large network-reduction power system models can be found in [22], [16], [46], [54], [64], [65].

1) Numerical Studies on Two Systems:

The numerical network-reduction BCU method has been tested on several power systems. The numerical simulation results presented in this section are a 50-generator, 145-bus power system which is a IEEE test system [65] and a 202-generator, 1293-bus power system. The type of faults are three-phase faults with fault locations at both generator and load buses. Both severe and mild faults are considered.

Table 3 displays the estimated critical clearing times of several faulted systems by using six different methods on the IEEE test system. In this study, the test system is modeled by the network-reduction power system model with classical generators. The six different methods are: the time-domain (numerical integration) method (ETMSP), the BCU method, the MOD method, the exit point method, the hybrid method and the mixed DEEAC method. The MOD method attempts to find the controlling u.e.p. based on the mode of disturbances. The hybrid method is a hybrid of a direct method and a time-domain method. The mixed DEEAC method is based on a dynamic equivalent equal area criterion. A description of each of these methods can be found in [36], [37], [50], [67], [74], [83]. The results from the time-domain method are used as a benchmark. The second line of Table 3 states that a three-phase fault occurs at bus 7 and the postfault system is the system with the transmission line between buses 6 and 7 tripped, due to the openings of circuit breakers at both ends of the line. The CCT estimated by the BCU method due to this type and location of fault with the way of 'clearing' the fault is 102 ms while the exact CCT obtained by the time-domain simulation method is 108 ms. The CCT estimated by the MOD method, the exit point method, the hybrid method and the mixed DEEAC method is 112.5, 112.5, 107.5, and 108 ms, respectively. Table 3 also lists the relative error of each method compared against the time-domain method. The sign ** in the Table 3 means that the corresponding method does not converge to a u.e.p. in that case. All these simulation results except for those by the BCU method display in Table 3 were taken from [26] and [67, pp. 203 and 235].

Table 5 Simulation Results of the 202-Generator, 1293-Bus Network-Reduction Power System with Classical Generator Models

Faulted Bus	Opened Line	CCT BCU	CCT ETMSP	Relative Error (%)
77	77-124	320	320	0
74	74-76	313	330	−5.10
75	75-577	212	210	0.95
136	136-103	260	260	0
248	248-74	133	160	−16.8
360	360-345	262	270	−2.90
559	559-548	197	210	−6.10
634	634-569	197	210	−6.10
661	661-669	103	120	−15.10
702	702-1376	214	220	−2.70
221	221-223	191	220	−13.10
175	175-172	269	270	−0.30
198	198-230	145	150	−3.30
245	245-246	224	230	−2.61
319	319-332	198	230	−13.90
360	360-362	262	270	−3.90

It should be pointed out that in these simulation results the BCU method consistently gives slightly conservative results in estimating CCT. These results are in compliance with the analytical results of the controlling u.e.p. method presented in Section V confirming that the critical energy value based on the controlling u.e.p. should give slightly conservative stability assessments if exact energy functions are used. The simulation results also reveal that the CCT's estimated by the other methods can be either overestimates or underestimates. Overestimating CCT is undesirable because it could lead to classifying an unstable case to be stable. Note that numerical energy functions were used in these simulations.

The numerical network-reduction BCU method is also applied to estimate the CCT of several faulted systems, modeled by the network-reduction, two-axis generator with a first-order exciter models. Table 4 lists some simulation results on the IEEE test system with 6 generators equipped with exciters. Table 6 lists some simulation results on the 202-generator, 1293-bus power system with the classical generator model. Two methods were used in these simulations: the time-domain method and the BCU method. The results from the time-domain method are used as a benchmark. Again, the BCU method consistently gives slightly conservative results in estimating CCT. These results are in compliance with the analytical results of the controlling u.e.p. method, despite the fact that numerical energy functions were used in these simulations.

B. Network-Preserving Power System Models

A numerical implementation of the conceptual BCU method for network-preserving power system models discussed in Section VII-F is presented below.

A Numerical Network Preserving BCU Method:

Step 1: From the (sustained) fault-on trajectory $(u(t), w(t), x(t), y(t), z(t))$ of the DAE system, detect the exit point (u^*, w^*, x^*, y^*) at which the projected trajectory $(u(t), w(t), x(t), y(t))$ reaches the first local maximum of the numerical potential energy function $U_{\text{num}}(\cdot,\cdot,\cdot,\cdot)$.

Step 2: Use the point (u^*, w^*, x^*, y^*) as the initial condition and integrate the postfault, dimension-reduction system (26) to the (first) local minimum of

$$\begin{aligned}&\left\|\frac{\partial}{\partial u}U(u,w,x,y)+g_1(u,w,x,y)\right\|\\&\quad+\left\|\frac{\partial}{\partial w}U(u,w,x,y)+g_2(u,w,x,y)\right\|\\&\quad+\left\|\frac{\partial}{\partial x}U(u,w,x,y)+g_3(u,w,x,y)\right\|\\&\quad+\left\|\frac{\partial}{\partial y}U(u,w,x,y)+g_4(u,w,x,y)\right\|.\end{aligned}$$

Let the local minimum be $(u_o^*, w_0^*, x_o^*, y_o^*)$.

Step 3: Use the point $(u_o^*, w_0^*, x_o^*, y_o^*)$ as the initial guess and solve the following set of nonlinear algebraic equations

$$\begin{aligned}&\left\|\frac{\partial}{\partial u}U(u,w,x,y)+g_1(u,w,x,y)\right\|\\&\quad+\left\|\frac{\partial}{\partial w}U(u,w,x,y)+g_2(u,w,x,y)\right\|\\&\quad+\left\|\frac{\partial}{\partial x}U(u,w,x,y)+g_3(u,w,x,y)\right\|\\&\quad+\left\|\frac{\partial}{\partial y}U(u,w,x,y)+g_4(u,w,x,y)\right\|=0.\end{aligned}$$

Let the solution be $(u_{co}^*, w_{co}^*, x_{co}^*, y_{co}^*)$.

Step 4: The controlling u.e.p. with respect to the fault-on trajectory $(u(t), w(t), x(t), y(t), z(t))$ of the DAE system is $(u_{co}^*, w_{co}^*, x_{co}^*, y_{co}^*, 0)$.

Steps 1–3 find the controlling u.e.p. of the artificial, dimension-reduction system and Step 4 relates the controlling u.e.p. of the dimension-reduction system to the controlling u.e.p. of the original system. In Step 2, the integration of the postfault dimension-reduction system can be replaced by the integration of the boundary-layer system of the postfault dimension-reduction system to accelerate the computational procedure. The remarks made on the numerical implementation of the conceptual network-reduction BCU method also apply to the above numerical network-preserving BCU method.

1) Numerical Studies on the IEEE Test System: The numerical network-preserving BCU method has also been tested on several power systems, modeled by a network-preserving, classical generator with static nonlinear load representations. The static nonlinear load model is a combination of constant power, constant impedance and constant current. The simulation results presented in this subsection are on the IEEE 50-generator, 145-bus test system and the 202-generator, 1293-bus system discuss in the previous subsection.

Table 6 Simulation Results of the 50-Machine, 145-Bus IEEE Test System Modeled by the Network-Preserving Power System with Classical Generators and Static Nonlinear Loads Comprised a Combination of 20% Constant Power, 20% Constant Current, and 60% Constant Impedance

Faulted Bus	Opened Line	CCT BCU Method	CCT ETMSP	Relative Error (%)
7	7-6	97	103	−5.8
59	59-72	208	222	−6.3
73	73-74	190	215	−11.8
112	112-69	235	248	−5.2
66	66-69	156	168	−7.1
115	115-116	288	292	−1.3
110	110-72	245	260	−5.7
101	101-73	232	248	−6.4
91	91-75	187	189	−1.1
6	6-1	153	170	−10.0
12	12-14	163	173	−5.8
6	6-10	162	177	−9.4
66	66-111	157	172	−9.7
106	106-74	170	186	−9.6
69	69-32	186	202	−7.9
69	69-112	110	118	−6.7
105	105-73	191	211	−9.4
73	73-75	194	210	−7.6
67	67-65	230	231	−0.4
59	59-103	221	223	−0.9
12	12-14, 12-14	156	167	−6.5
105	105-73, 105-73	110	118	−6.7
66	66-8, 66-8	167	174	−4.0
66	66-111, 66-111, 66-111	70	80	−12.5
73	73-26, 73-72, 73-82, 73-101	192	212	−9.4
73	73-69, 73-75, 73-96, 73-109	182	190	−4.2

Table 6 displays the estimated CCT of the IEEE 50-generator, 145-bus test system with different locations of three-phase faults using the time-domain method and the network-preserving BCU method. The load model used in this numerical study is a combination of 20% constant power, 20% constant current, and 60% constant impedance. The network-preserving BCU method is also applied to a nonlinear static load model, which is a combination of 20% constant power, 20% constant current, and 60% constant impedance. Table 7 contains the simulation results of the 202-generator, 1293-bus. The simulation results are the estimated CCT's of the system with different locations of three-phase faults using the time-domain method and the BCU method with 1) constant impedance loads, and 2) a nonlinear static load which is a combination of 20% constant power, 20% constant current, and 60% constant impedance. Again, the computational performance of the network-preserving BCU method is that it consistently gives slightly conservative results in estimating CCT which is in compliance with the controlling u.e.p. method, despite the fact that numerical energy functions were used in these simulations. Moreover, the computational performance of the network-preserving BCU method seems to be very consistent when applied to different static load models.

Table 7 Simulation Results of the 202-Machine, 1293-Bus System Modeled by the Network-Preserving Power System with (1) Classical Generators and Constant Impedance Load Models, and (2) Classical Generators and Static Nonlinear Loads Comprised a Combination of 20% Constant Power, 20% Constant Current, and 60% Constant Impedance

Faulted Bus	Opened Line	LOAD(1)			LOAD(2)		
		CCT ETMSP	CCT BCU Method	Relative Error (%)	CCT ETMSP	CCT BCU Method	Relative Error (%)
77	77-124	0.325	0.320	−1.6	0.325	0.320	−1.6
74	74-76	0.343	0.313	−9.7	0.336	0.305	−9.2
75	75-577	0. 210	0. 212	−0.9	0. 210	0.212	−0.9
136	136-103	0.262	0. 260	−0.7	0.262	0.260	−0.7
248	248-74	0.165	0.160	−3.1	0.165	0.160	−3.1
360	360-345	0.273	0.262	−4.1	0.271	0.261	−3.6
559	559-548	0.215	0.197	−9.3	0.212	0.190	−11.3
634	634-569	0.212	0.197	−7.1	0.205	0.188	−9.2
661	661-669	0.123	0.103	−6.3	0.123	0.103	−16.3
702	702-1376	0.233	0.224	−3.8	0.230	0.222	−3.4
221	221-223	0.220	0.214	−3.2	0.216	0.209	−3.2
175	175-172	0.276	0.269	−3.5	0.272	0.262	−3.6
198	198-230	0.156	0.145	−7.1	0.155	0.145	−6.4
245	245-246	0.230	0. 224	−2.6	0.228	0.220	−3.5
319	319-332	0.230	0.198	−13.9	0.229	0.198	−13.5
360	360-362	0.272	0.262	−3.6	0.272	0.261	−4.1

C. A Sensitivity-Based BCU Method

Quite often, power system operators need to cope with the following situation: for a given power system with a given contingency, called the base case, if some of the parameters in the system change (due to a disturbance, perhaps), called the new case, one must know how these changes affect the system stability as quickly as possible. Also, there is a great need of a fast, yet accurate method to determine the transient stability-constrained loading limits, power transfer limits and, furthermore, to decide how to make changes in the parameters, such as generation rescheduling, and load shedding in order to improve system transient behaviors.

Numerous previous methods [31], [59], [73], [82] have attempted to use the sensitivity of energy functions to changes in system parameters to determine the stability limits of systems. It is assumed in these methods that the mode of the controlling u.e.p. does not change. In general, this assumption may not be true for every case. A counterexample of the assumption on a 50-generator, 145-bus system was provided in [16].

The sensitivity-based BCU method also allows one to quickly determine the extent to which one may change real power generations in the system before jeopardizing its transient stability, or how much change is necessary in order to gain stability. The chief advantage of the sensitivity-based BCU method is that it does not make the assumption that the new case will have roughly the same controlling u.e.p. as the base case. The main idea behind the sensitivity-based BCU method is that the values of the state variables at the fault clearing time, X_{cl}, (i.e., the initial state of the postfault system) and at the exit point, X_e, (of the artificial, dimension-reduction system) can be quickly estimated when changes are made to the parameters of the base case to which the BCU method has already been applied. The controlling u.e.p. of the new case is then found following Steps 2–4 of the BCU method.

IX. Practical Demonstrations

This section summarizes some practical demonstrations of using direct methods and the BCU method for on-line transient stability assessments on two power systems. The role of the BCU method is to determine critical energy values for direct methods. The first demonstration to be discussed involves a prototype of an on-line transient stability assessment function which was tested on a 161-generator power system model at the Northern States Power Company (NSP) under the sponsorship of EPRI [52]. This application consists of two major components: a contingency screen program made up of a sequence of filters based on the BCU method and an on-line transient simulation program based on EPRI's Extended Transient and Midterm Stability Program (ETMSP). A framework for on-line dynamic contingency screening, selection, and ranking is presented in Fig. 23.

In the prototype, a sequence of three contingency filters is applied to a list of contingencies. These three contingency filters are based on the three steps of the BCU method. The first filter, based on step one of the BCU method, is the fastest one. It uses the exit point on the stability boundary of the dimension-reduction system as an approximation for computing the energy margin. The second filter uses the minimum semigradient point, which is the second step of the BCU method. The third and most exact filter uses the controlling u.e.p. to compute the critical energy, which is the third step of the BCU method. Contingencies which are definitely stable are dropped from further analysis at each filter step. The computations for each contingency are cumulative through the three filters, avoiding the need to

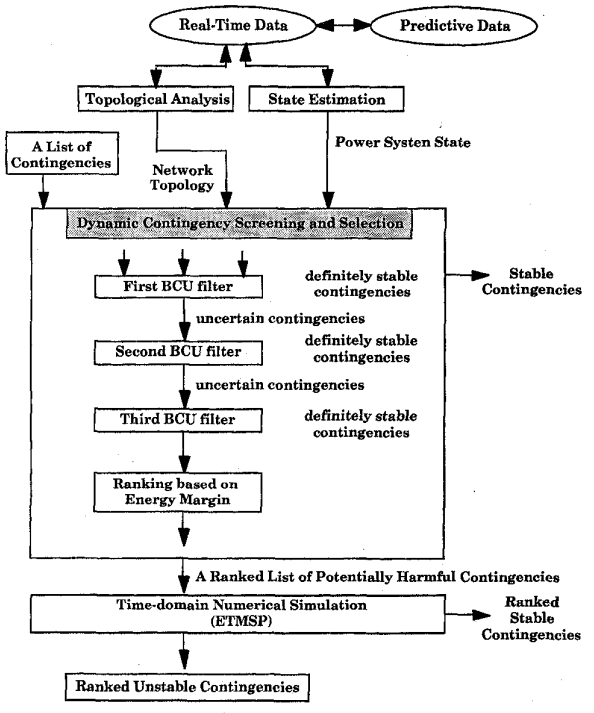

Fig. 23. A framework for on-line dynamic contingency screening, selection and ranking.

repeat computations. Cases identified as requiring further analysis are sent to the ETMSP for detailed time-domain assessments. Each filter is intended to be conservative and has been tested to be so (i.e., no unstable cases are misclassified as stable). The speed up achieved by using the BCU filters, developed by the Empros and Iowa State University, is more than six times faster than what would have been required to run a time-domain simulation on each contingency.

The prototype has been integrated into the control center at NSP and is intended to allow increased MW transfers from the north. The program has undergone an evaluation by NSP engineers and operators and is expected to provide significant dollar savings when completed as a production program.

Direct methods have also been demonstrated under EPRI sponsorship at the control center of Ontario Hydro [46]. This program is an on-line transfer limit calculation based on the BCU method. The program uses a time-domain simulation program supplied by Ontario Hydro to compute the exit point at which the projected fault-on trajectory crosses the stability boundary of the artificial, dimension-reduction system. From there, a minimum gradient point search and a calculation of the controlling u.e.p. are completed. The results of the program include energy margins and sensitivities to power system parameters. This program has been integrated into the energy management system at Ontario Hydro and demonstrated to the industry at a workshop in December 1993. The program was validated using off-line analysis with a simulation program.

Previous EPRI-sponsored project results have shown that direct stability analysis is feasible for large power systems and it has several important applications. The EPRI software-DIRECT is a production-grade computer package for direct stability analysis of large-scale power systems. The latest version of DIRECT 4.0 uses the network-preserving BCU method to compute the critical energy.

X. Perspective

Direct methods provide advantages which make them a good complement to the traditional time-domain simulation approach. The current direction of development is to include direct methods within the simulation programs themselves. For example, the energy margin and its sensitivity to certain power system parameters are an effective complement which can significantly reduce the number of simulations required to compute power transfer limits. In the future one should expect direct methods will become components of commercial grade transient stability simulation programs. Yet, direct methods will need some improvements to be used as a reliable complement to the traditional time-domain simulation approach.

Direct methods have been based on the energy function theory for nonlinear autonomous systems. As such, there are several limitations on the applications of current direct methods; some of them are inherent to direct methods. These limitations may be classified as: the modeling limitation, the scenario limitation, the function limitation, and the accuracy limitation. Roughly speaking, the modeling limitation stems from the requirement of having an energy function for a given power system model, but not every power system model has an energy function associated with it [48], [20]. The scenario limitation comes from the requirement of the initial condition of the postfault system, which must be obtained using the time-domain approach and which may not be available beforehand. This is an inherent limitation in direct methods. The function limitation shows that in theory several of the current direct methods are only applicable to power system models described by pure differential equations and work only for first-swing transient stability analysis.

A major limitation of direct methods in the past has been the simplicity of the models used in various direct method implementations in software programs. Recent work in this area has overcome much of this limitation. As to the function limitation stipulating that direct methods are only applicable to first swing instability, the direct method based on the controlling u.e.p. method has now been shown in this paper to provide useful information for identifying multi-swing unstable cases. Regarding the accuracy and reliability of direct methods, this limitation can be significantly improved by the work (BCU method) presented in this paper for network-preserving power system models. In practical applications, the controlling u.e.p. method, in conjunction with the BCU method, has shown promise as a tool for fast approximate contingency screening (thereby improving performance) and efficiently computing operating limits.

The scenario limitation of direct methods still needs to be solved.

Given a power system stability model, the existence of an energy function and the ability to compute the controlling u.e.p. are essential for direct stability analysis of the underlying model. A systematic procedure of constructing energy functions for both network-reduction and network-preserving power system models is proposed in this paper. The BCU method extensively described in this paper is a systematic method of computing the controlling u.e.p. for large-scale power systems. It explores the special structure of the underlying model so as to define an artificial, dimension-reduction system which can capture all of the equilibrium points on the stability boundary of the underlying system. The BCU method then finds the controlling u.e.p. of the original system via the controlling u.e.p. of the dimension-reduction system which is much easier to find than that of the original system. Given a power system stability model with certain properties, there exists a corresponding version of the BCU method. The paper has demonstrated, through an exposition of the BCU method, that analytical results can sometimes lead to the development of reliable yet fast solution algorithms for solving problems. This further enhances the authors' belief that solving practical problems efficiently can be accomplished through a thorough understanding of the underlying theory, in conjunction with exploring the features of the practical problem under study.

This paper has also presented a general framework for the BCU method and developed a theoretical foundation for the BCU method for both the network-reduction and the network-preserving power system stability models. In addition to demonstrating its practical applications to on-line transient stability analysis, sufficient conditions for the BCU method to find the correct controlling u.e.p. relative to a given fault have also been derived. From a practical viewpoint, it would be usefulto know whether or not these sufficient conditions are always satisfied for practical large-scale power systems. There are certainly other avenues we may explore in order to improve the reliablity, accuracy, and computational speed of the BCU method. For instance, the issue of how to find an optimal artificial dimension-reduction system such that, in addition to satisfying the static and dynamic properties presented in Section VI-C, it also has a desired level of smoothness on its stability boundary or it offers much milder sufficient condition for the BCU method to work (e.g., it removes part of the requirement of the one-parameter transversality condition).

A stability problem causing great concerns in power industry is the voltage-dip problem. This problem can be stated as follows: following a disturbance (event disturbance or load disturbance), whether or not the underlying power system will settle down to an acceptable steady-state (in the context of frequency and voltage) and during the transient, the system voltage will not dip to un-acceptable values (see Fig. 24). The problem is particularly significant in the current operating condition of the North America's interconnected power network whose systems are now

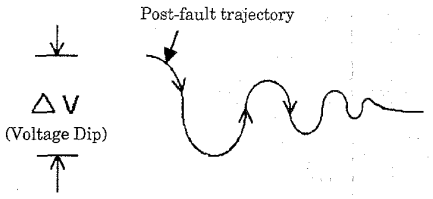

Fig. 24. Following a disturbance (event disturbance or load disturbance), whether or not the underlying power system will settle down to an acceptable steady-state and during the transient, the system voltage will not dip to un-acceptable values.

operated very close to their security limits. Mathematically, the voltage dip problem can be stated as follows: given a set of nonlinear equations with an initial condition, determine whether or not the ensuing trajectories will settle down to a desired steady-state without resort to explicit numerical integrations of a whole set of nonlinear equations; furthermore, one wants to know whether during the transient, part of the state variables (related to voltage magnitudes at load buses) drop below a certain value, say 0.9 p.u. Alternatively, from a nonlinear system viewpoint, the problem can be stated in the following way: given a set of nonlinear equations with an initial condition, determine 1) whether or not the initial condition lies inside the stability region (region of attraction) of a desired stable equilibrium point and, 2) whether or not the projected system trajectory on the subspace spanned by the voltage magnitudes at load buses does not fall below a certain value. Obviously, the voltage-dip problem is very unique and challenging. It is imperative to extend the functionality of direct methods for solving the voltage-dip problems.

Further improvements in direct methods' limited modeling capability are desirable, especially to include an appropriate dynamic load modeling in the model. It is well known that inaccurate load modeling can lead to a power system operating in modes that result in actual system collapse or separation. Accurate load models capturing load behaviors during dynamics are therefore necessary for more precise calculations of power system controls and stability limits. Most of the load models used in direct methods are limited to the so-called static load models, where loads are represented as constant impedance, constant current, constant MVA, or some combinations of these three. These static load models may not adequately capture load behaviors during transient. Hence, it may prove rewarding to show that direct methods can be extended to structure-preserving stability models with sufficiently detailed load models (more accurate static load models or even adequate dynamic load models) and generator models with adequate nonlinear representations.

In recent years, practical experience has shown that a power system may become unstable ten to thirty seconds after a disturbance, even if it is stable in transient states. The power system is short-term stable and midterm unstable. One mechanism that may contribute to this phenomenon is that the initial state of the postfault system lies inside the stability region of the short-term power system model but

lies outside the stability region of the midterm power system model [15]. This points out the necessity of extending direct methods for midterm power system models. In this regard, it may prove useful to develop general functions (more general than the energy function) such that any nonlinear system having such a function has the following dynamic properties: 1) the ω-limit set of any of its bounded trajectories consists only of equilibrium points and limit cycles, and 2) the function is nonincreasing along its trajectories. Such a development will allow one to apply direct methods to detailed power system models whose stability boundaries contain equilibrium points and limit cycles. An example of such a model can be found in [75].

Due to the upcoming practice of power wheeling and open access to transmission systems, the utilities are more often concerned with determining the limiting power transfer across a boundary or the limits on the real power generation sent out of a power station. This concern coupled with the need to share full utilization of transmission among utilities for economic transfer have made the problem associated with transient-stability constrained transfer limits a pressing issue. The determination of power transfer limits becomes much more important than ever. Direct methods should be capable of providing such information more timely and readily than the conventional time-domain simulation approach. Extension of direct methods in this direction will be welcome.

The major breakthroughs presented in this paper include a solid mathematical foundation for direct methods, development of a systematical procedure for constructing energy functions for both network-reduction and network-preserving power system models, development of BCU methods for computing the controlling u.e.p. for network-preserving models and practical demonstrations of on-line stability assessments based on the controlling u.e.p. method in conjunction with the BCU method. The remaining hurdles include the resolution of detailed modeling involving high-level nonlinearity limitations in loads and generators and the removal of the scenario limitation.

ACKNOWLEDGMENT

The authors wish to express appreciation to Dr. C. S. Wang and Dr. C. Jing of Cornell University for their useful discussions.

REFERENCES

[1] R. Abraham, J. E. Marsden, and T. Ratiu, "Manifolds, tensor analysis, and applications," in *Applied Mathematical Sciences,* vol. 75. New York: Springer-Verlag, 1988.

[2] M. M. Abu-Elnaga, M. A. El-Kady, and R. D. Findlay, "Sparse formulation of the transient energy function method using sparse formulation to large-scale power systems," *IEEE Trans. Power Syst.,* vol. 3, pp. 1648–1654, Dec. 1988.

[3] ——, "Stability assessment of highly stressed power systems using sparse formulation of the direct method," *IEEE Trans. Power Syst.,* vol. 3, pp. 1655–1661, Dec. 1988.

[4] P. M. Anderson and A. A. Fouad, *Power System Control and Stability.* New York: IEEE Press, 1994.

[5] A. Arapostathis, S. S. Sastry, and P. Varaiya, "Global analysis of swing dynamics," *IEEE Trans. Circ. and Syst.,* vol. CAS-29, pp. 673–679, 1982.

[6] D. K. Arrowsmith and C. M. Place, *An Introduction to Dynamical Systems.* Cambridge, UK: Cambridge Univ. Press, 1990.

[7] T. Athay, R. Podmore, and S. Virmani, "A practical method for the direct analysis of transient stability," *IEEE Trans. Power Apparatus and Syst.,* vol. PAS-98, no. 2, pp. 573–584, 1979.

[8] P. D. Aylett, "The energy integral-criterion of transient stability limits of power systems," *Proc. IEE,* vol. 105c, no. 8, pp. 527–536, Sept. 1958.

[9] A. R. Bergen and D. J. Hill, "A structure preserving model for power system stability analysis," *IEEE Trans. Power Apparatus and Syst.,* vol. PAS-100, pp. 25–35, 1981.

[10] A. R. Bergen, D. J. Hill, and C. L. De Marco, "Lyapunov function for multimachine power systems with generator flux decay and voltage dependent loads," *Int. J. Electrical Power and Energy Syst.,* vol. 8, no. 1, pp. 2–10, 1986.

[11] K. E. Brenan, S. L. Campbell, and L. R. Petzold, *Numerical Solution of Initial-Value Problems in Differential-Algebraic Equations.* Amsterdam: Elsevier, 1989.

[12] U. Di Caprio, "Accounting for transfer conductance effects in Lyapunov transient stability analysis of a multimachine power system," *Int. J. Electrical Power and Energy Syst.,* vol. 8, no. 1, pp. 27–41, 1986.

[13] H. D. Chiang, "Study of the existence of energy functions for power systems with losses," *IEEE Trans. Circ. and Syst.,* vol. 36, pp. 1423–1429, Nov. 1989.

[14] ——, "Analytical results on the direct methods for power system transient stability analysis," in *Control and Dynamic Systems: Advances in Theory and Application.* New York: Academic, 1991, vol. 43, pp. 275–334.

[15] ——, "The BCU method for direct stability analysis of electric power systems: Theory and applications," J. Chow, P. V. Kokotovic, and R. J. Thomas, Eds., in *Systems Control Theory for Power Systems,* vol. 64 of *IMA Volumes in Mathematics and Its Applications.* New York: Springer-Verlag, 1995, pp. 39–94.

[16] H. D. Chiang and C. C. Chu, "Theoretical foundation of the BCU method for direct stability analysis of network-reduction power system model with small transfer conductances," *IEEE Trans. on Circuits and Systems-I: Fundamental Theory and Applications,* vol. CAS-42, no. 5, pp. 252–265, May 1995.

[17] H. D. Chiang and L. Fekih-Ahmed, "On the direct method for transient stability analysis of power system structure preserving models," in *IEEE Int. Symp. on Circ. and Syst.,* 1992, pp. 2545–2548.

[18] H. D. Chiang, M. W. Hirsch, and F. F. Wu, "Stability region of nonlinear autonomous dynamical systems," *IEEE Trans. Auto. Control,* vol. 33, pp. 16–27, Jan. 1988.

[19] H. D. Chiang and J. S. Thorp, "The closest unstable equilibrium point method for power system dynamic security assessment," *IEEE Trans. Circ. and Syst.,* vol. 36, pp. 1187–1120, Sept. 1989.

[20] H. D. Chiang, F. F. Wu, and P. P. Varaiya, "Foundations of direct methods for power system transient stability analysis," *IEEE Trans. Circ. and Syst.,* vol. CAS-34, pp. 160–173, Feb. 1987.

[21] ——, "Foundations of the potential energy boundary surface method for power system transient stability analysis," *IEEE Trans. Circ. and Syst.,* vol. 35, pp. 712–728, June 1988.

[22] ——, "A BCU method for direct analysis of power system transient stability," *IEEE Trans. Power Syst.,* vol. 9, pp. 1194–2000, Aug. 1994.

[23] C. C. Chu, "Transient dynamics of electric power systems: Direct stability assessment and chaotic motions," Ph.D. dissertation, Cornell Univ., Ithaca, NY, Jan. 1996.

[24] C. C. Chu and H. D. Chiang, "Analytical energy functions for electric power systems with detailed generator and load models: Framework and developments," to be published in *IEEE Trans. Circ. and Syst.-I: Fund. Theory and Applic.*

[25] L. O. Chua and A. C. Deng, "Impasse points-part ii: Analytic aspects," *Int. J. Circuit Theory,* vol. 17, no. 3, pp. 271–289, 1989.

[26] CIGRE Task Force Rep., "Assessment of practical fast transient stability methods," Convener S. Geeves, June 1992.

[27] R. H. Craven and M. R. Michael, "Load characteristic measurements and representation of loads in the dynamic simulation of the Queensland power system," in *1983 CIGRE and IFAC Symp.,* Florence, 1983, pp. 39–83.

[28] C. L. De Marco and A. R. Bergen, "Application of singular perturbation techniques to power system transient stability

analysis," in *IEEE Int. Symp. on Circ. and Syst.,* 1984, pp. 597–601.
[29] ——, "A security measure for random load disturbances in nonlinear power system models," *IEEE Trans. Circ. and Syst.,* vol. CAS-34, pp. 1546–1557, 1987.
[30] A. H. El-Abiad and K. Nagappan, "Transient stability regions for multi-machine power systems," *IEEE Trans. Power Apparatus and Syst.,* vol. PAS-85, pp. 169–179, 1966.
[31] M. A. El-kady *et al.,* "Dynamic security assessment utilizing the transient energy function method," *IEEE Trans. Power Syst.,* vol. PS-1, pp. 284–291, Mar. 1986.
[32] D. N. Ewart, "Whys and wherefores of power system blackouts," *IEEE Spectrum,* vol. 15, pp. 36–41, 1978.
[33] L. Fekih-Ahmed, "Theoretical results on the stability regions and bifurcations of nonlinear dynamical systems and their applications to electric power system analysis," Ph.D. dissertation, Cornell Univ., Ithaca, NY, Aug. 1991.
[34] R. Fischl, F. Mercede, F. F. Wu, and H. D. Chiang, "Comparison of dynamic security indices based on direct methods," *Int. J. Electrical Power and Energy Syst.,* vol. 10, no. 4, pp. 210–232, 1988.
[35] A. A. Fouad and S. E. Stanton, "Transient stability of a multimachine power systems. Part i: Investigation of system trajectories," *IEEE Trans. Power Apparatus and Syst.,* vol. PAS-100, pp. 3408–3414, July 1981.
[36] A. A. Fouad and V. Vittal, "The transient energy function method," *Int. J. Electrical Power and Energy Syst.,* vol. 10, no. 4, pp. 233–246, 1988.
[37] ——, *Power System Transient Stability Analysis: Using the Transient Energy Function Method.* Englewood Cliffs, NJ: Prentice-Hall, 1991.
[38] G. E. Gless, "Direct method of Lyapunov applied to transient power system stability," *IEEE Trans. Power Apparatus and Syst.,* vol. PAS-85, pp. 164–179, 1966.
[39] J. Guckenheimer and P. Holmes, *Nonlinear Oscillations, Dynamical Systems, and Bifurcations of Vector Fields,* Applied Mathematical Sciences Series No. 42. New York: Springer-Verlag, 1983.
[40] U. Guadra, "A general Liapunov function for multi-machine power systems with transfer conductances," *Int. J. Control,* vol. 21, no. 2, pp. 333–343, 1975.
[41] D. J. Hill and I. M. Y. Mareels, "Stability theory for differential/algebraic systems with application to power systems," *IEEE Trans. Circ. and Syst.,* vol. 37, pp. 1416–1422, 1990.
[42] M. Hirsch and S. Smale, *Differential Equations, Dynamical Systems and Linear Algebra.* New York: Academic, 1974.
[43] I. A. Hiskens and D. J. Hill, "Energy functions, transient stability and voltage behavior in power systems with nonlinear loads," *IEEE Trans. Power Syst.,* vol. 4, pp. 1525–1533, 1989.
[44] N. Kakimoto, Y. Ohsawa, and M. Hayashi, "Transient stability analysis of electric power system via lure-type Lyapunov function," *Trans. IEE of Japan,* vol. 98, pp. 566–604, 1978.
[45] H. K. Khalil, *Nonlinear Systems.* New York: Macmillan, 1992.
[46] J. Kim, "On-line transient stability calculator," Final Rep. RP2206-1, EPRI, Palo Alto, CA, Mar. 1994.
[47] D. H. Kuo and A. Bose, "A generation rescheduling method to increase the dynamics security of power systems," *IEEE Trans. Power Syst.,* vol. 10, pp. 68–76, Jan. 1995.
[48] H. G. Kwatny, L. Y. Bahar, and A. K. Pasrija, "Energy-like Lyapunov functions for power system stability analysis," *IEEE Trans. Circ. and Syst.,* vol. CAS-32, pp. 1140–1149, Nov. 1985.
[49] A. Llamas *et al.,* "Clarifications of the BCU method for transient stability analysis," *IEEE Trans. Power Syst.,* vol. 10, pp. 210–219, Jan. 1995.
[50] W. W. Lemmon, K. R. C. Mamandur, and W. R. Barcelo, "Transient stability prediction and control in real-time by quasi-unstable equilibrium point (QUEP) methods," *IEEE Trans. Power Syst.,* vol. 4, pp. 44–52, Jan. 1989.
[51] P. C. Magnusson, "Transient energy method of calculating stability," *AIEE Trans.,* vol. 66, pp. 747–755, 1947.
[52] G. A. Maria, C. Tang, and J. Kim, "Hybrid transient stability analysis," *IEEE Trans. Power Syst.,* vol. 5, pp. 384–393, Feb. 1990.
[53] H. Miyagi and A. R. Bergen, "Stability studies of multimachine power systems with the effects of automatic voltage regulators," *IEEE Trans. Auto. Contr.,* vol. AC-31, pp. 210–215, 1986.
[54] S. Mokhtari, "Analytical methods for contingency selection and ranking for dynamic security assessment," Final Rep. RP3103-3, EPRI, Palo Alto, CA, May 1994.
[55] N. Narasimhamurthi, "On the existence of energy functions for power systems with transmission losses," *IEEE Trans. on Circuits and Systems,* vol. CAS-31, pp. 199–203, 1984.
[56] N. Narasimhamurthi and M. R. Musavi, "A general energy function for transient stability analysis of power systems," *IEEE Trans. Circ. and Syst.,* vol. CAS-31, pp. 637–645, 1984.
[57] R. E. J. O'Malley, *Singular Perturbation Methods for Ordinary Differential Equations,* vol. 89, *Applied Mathematical Sciences,* Springer-Verlag, 1991.
[58] K. R. Padiyar and K. K. Ghosh, "Direct stability evaluation of power systems with detailed generator models using structure-preserving energy functions," *Int. J. Electrical Power and Syst.,* vol. 11, no. 1, pp. 47–56, 1989.
[59] M. A. Pai, *Power System Stability.* Amsterdam: North-Holland, 1981.
[60] M. A. Pai, *Energy Function Analysis for Power System Stability.* Boston: Kluwer Academic Publishers, 1989.
[61] M. A. Pai, P. W. Sauer, and K. D. Demaree, "Direct methods of stability analysis in dynamic security assessment," in *Proc. 9th IFAC World Congress,* Budapest, July 1984.
[62] J. Palis and W. De Melo, *Geometric Theory of Dynamical Systems: An Introduction.* New York: Spring-Verlag, 1982.
[63] F. S. Prabhakara and A. H. El-Abiad, "A simplified determination of stability regions for Lyapunov method," *IEEE Trans. Power Apparatus and Syst.,* vol. PAS-94, pp. 672–689, 1975.
[64] F. A. Rahimi, "Evaluation of transient energy function method software for dynamic security analysis," Final Rep. RP 4000-18, EPRI, Palo Alto, CA, Dec. 1990.
[65] F. A. Rahimi, M. G. Lauby, J. N. Wrubel, and K. L. Lee, "Evaluation of the transient energy function method for on-line dynamic security assessment," *IEEE Trans. Power Syst.,* vol. 8, pp. 497–507, 1993.
[66] IEEE Committee Rep., "Excitation systems models for power system studies," *IEEE Trans. Power Apparatus and Syst.,* vol. PAS-97, pp. 494–509, 1981.
[67] IEEE Committee Rep., "Transient stability test systems for direct stability methods," *IEEE Trans. Power Syst.,* vol. 7, pp. 37–43, 1992.
[68] M. Ribbens-Pavella and F. J. Evans, "Direct methods for studying dynamics of large-scale electric power systems—A survey," *Automatica,* vol. 21, no. 1, pp. 1–21, 1985.
[69] M. Ribbens-Pavella and P. G. Murthy, *Transient Stability of Power Systems: Theory and Practice.* New York: Wiley, 1994.
[70] M. Ribbens-Pavella, P. G. Murthy, and J. L. Horward, "The acceleration approach to practical transient stability domain estimation in power systems," in *IEEE Control and Decision Conf.,* San Diego, CA, Dec. 1981, vol. 1, pp. 471–476.
[71] C. Robinson, *Dynamical Systems: Stability, Symbolic Dynamics, and Chaos.* Boca Raton, FL: CRC, 1994.
[72] H. Sasaki, "An approximate incorporation of fields flux decay into transient stability analysis of multi-machine power systems by the second method of Lyapunov," *IEEE Trans. Power Apparatus and Syst.,* vol. PAS-98, pp. 473–483, Feb. 1979.
[73] S. Sastry and C. A. Desoer, "Jump behavior of circuits and systems," *IEEE Trans. Circ. and Syst.,* vol. CAS-28, pp. 1109–1124, Dec. 1981.
[74] S. Sastry and P. Varaiya, "Hierarchical stability and alert state steering control of interconnected power systems," *IEEE Trans. Circ. and Syst.,* vol. CAS-27, pp. 1102–1112, 1980.
[75] P. W. Sauer *et al.,* "Trajectory approximation for direct energy methods that use sustained faults with detailed power system models," *IEEE Trans. Power Syst.,* vol. 4, pp. 499–506, Feb. 1989.
[76] P. W. Sauer, K. D. Demaree, and M. A. Pai, "Stability limited load supply and interchange capability," *IEEE Trans. Power Apparatus and Syst.,* vol. PAS-102, pp. 3637–3643, 1983.
[77] C. K. Tang, C. E. Graham, M. El-Kady, and R. T. H. Alden, "Transient stability index from conventional time domain simulation," *IEEE Trans. Power Systems,* vol. 9, pp. 1524–1530, Mar. 1994.
[78] N. A. Tsolas, A. Arapostathis, and P. P. Varaiya, "A structure preserving energy function for power system transient stability analysis," *IEEE Trans. Circ. and Syst.,* vol. CAS-32, pp. 1041–1049, 1985.

[79] P. P. Varaiya, F. F. Wu, and R.-L. Chen, "Direct methods for transient stability analysis of power systems: Recent results," *Proc. IEEE,* vol. 73, pp. 1703–1715, 1985.
[80] V. Venkatasubramanian, H. Schättler, and J. Zaborszky, "A taxonomy of the dynamics of the large power system with emphasis on its voltage stability," in *Proc., Bulk Power System Voltage Phenomena II: Voltage Stability and Security: An International Seminar,* Deep Lake, MD, 1991, pp. 9–52.
[81] ——, "Voltage dynamics: Study of a generator with voltage control, transmission, and matched MW load," *IEEE Trans. Autom. Contr.,* vol. 37, pp. 1717–1732, Nov. 1992.
[82] ——, "Feasibility regions and bifurcation boundaries in constrained systems such as the large power system," to be published in *IEEE Trans. Auto. Control.*
[83] M. Vidyasagar, *Nonlinear Systems Analysis,* Networks Series. Englewood Cliffs, NJ: Prentice-Hall, 1978.
[84] S. Wiggins, *Introduction to Applied Nonlinear Dynamical Systems and Chaos,* vol. 2 of *Texts in Applied Mathematics.* New York: Springer-Verlag.
[85] J. L. Willems, "Direct methods for transient stability studies in power system analysis," *IEEE Trans. Auto. Contr.,* vol. AC-16, pp. 332–341, Apr. 1971.
[86] Y. Xue, Th. Van Custem, and M. Ribbens-Pavella, "Real-time analytic sensitivity method for transient security assessment and prevent control," *Proc. IEEE,* Pt. C, vol. 135, pp. 107–117, Mar. 1988.
[87] ——, "Extended equal area criterion justifications, generalizations, applications," *IEEE Trans. Power Syst.,* vol. 4, pp. 44–52, Jan. 1989.
[88] Y. Xue *et al.,* "Extended equal area criterion revised," *IEEE Trans. Power Syst.,* vol. PS-7, pp. 1012–1022, 1992.
[89] H. Yee and B. D. Spalding, "Transient stability analysis of multimachine power systems by the method of hyperplanes," *IEEE Trans. Power Apparatus and Syst.,* vol. PAS-96, pp. 276–284, Jan. 1977.
[90] J. Zaborszky, G. Huang, B. Zheng, and T. C. Leung, "On the phase portrait of a class of large nonlinear dynamic systems such as the power system," *IEEE Trans. Auto. Contr.,* vol. 33, pp. 4–15, Jan. 1988.

Hsiao-Dong Chiang (Senior Member, IEEE) received the B.S. and M.S. degrees in electrical engineering from the National Taiwan University, Taipei, Taiwan, and the Ph.D. degree in electrical engineering and computer sciences from the University of California at Berkeley.

He is currently an Associate Professor of Electrical Engineering at Cornell University, Ithaca, NY. He was an Associate Editor of the IEEE TRANSACTIONS ON CIRCUITS AND SYSTEMS from 1990 to 1991, and is currently Associate Editor for Express Letters of the IEEE TRANSACTIONS ON CIRCUITS AND SYSTEMS—I: FUNDAMENTAL THEORY AND APPLICATIONS. His research interests include the development of theoretical foundations and analytical tools for the analysis and control of physical systems, such as power and control systems, and the use of this work to achieve valuable and practical results.

Dr. Chiang received the Engineering Research Initiation Award in 1988 and the Presidential Young Investigator Award in 1989, both from the National Science Foundation. In 1990 he was selected by a Cornell Merrill Presidential Scholar as the faculty member who had the most influence on that student's education at Cornell.

Chia-Chi Chu (Student Member, IEEE) was born in Taipei, Taiwan, ROC, on September 4, 1965. He received the B.S. and M.S. degrees in electrical engineering from the National Taiwan University, Taipei, Taiwan, in 1987 and 1989, respectively. He is currently working toward the Ph.D. degree in electrical engineering (with a minor in applied mathematics) at Cornell University, Ithaca, NY. His research interests are in the applications of nonlinear dynamical system theory, including energy function, bifurcation, and chaos, for analyzing the dynamical behaviors of bulk electric power systems.

Mr. Chu is a student member of SIAM.

Gerry Cauley (Senior Member, IEEE) received the B.S. degree in electrical engineering from the US Military Academy at West Point, the M.S. degree in nuclear engineering from the University of Maryland, and the M.B.A. degree from Loyola College, Baltimore, MD.

He is presently the Manager of the Power Systems Planning and Operations Target of the Power Delivery Group, Electric Power Research Institute (EPRI), Palo Alto, CA. He is responsible for creating research strategies and developing products for use in power system control center and in power system planning. He has served as a project manager at EPRI and also serves as its liaison to the NERC Operating Committee. Before joining EPRI in 1991, he worked for General Physics Corporation from 1980 to 1990 as a Manager of Training Services for Power System Operations. He initially joined General Physics as a nuclear engineer conducting nuclear power plant training. From 1975 to 1980 he served in the Army Corps of Engineers as a Construction Engineer and as a Supervisor at a power generation training center.

Mr. Cauley is a Professional Engineer in the Commonwealth of Virginia. He is active in numerous IEEE task forces and working groups related to system operations and control centers.